JANUARY 2021 M.Sc. in Electrical and Electronics Engineering MEHMET FATİH ÇAKAR

REPUBLIC OF TURKEY

GAZİANTEP UNIVERSITY

GRADUATE SCHOOL OF NATURAL & APPLIED SCIENCES

IDENTIFICATION OF MECHANICAL BACKLASH IN ELECTROMECHANICAL SYSTEMS FOR CONTROL PURPOSES

M.Sc. THESIS

IN

ELECTRICAL AND ELECTRONICS ENGINEERING

BY

MEHMET FATİH ÇAKAR

JANUARY 2021

IDENTIFICATION OF MECHANICAL BACKLASH IN ELECTROMECHANICAL SYSTEMS FOR CONTROL PURPOSES

M.Sc. Thesis

in

Electrical and Electronics Engineering

Gaziantep University

Supervisor

Assoc. Prof. Dr. Tolgay KARA

by

Mehmet Fatih ÇAKAR

January 2021

I hereby declare that all information in this document has been obtained and presented in accordance with academic rules and ethical conduct. I also declare that, as required by these rules and conduct, I have fully cited and referenced all material and results that are not original to this work.

Mehmet Fatih ÇAKAR

ABSTRACT

IDENTIFICATION OF MECHANICAL BACKLASH IN ELECTROMECHANICAL SYSTEMS FOR CONTROL PURPOSES

ÇAKAR, Mehmet Fatih
M.Sc. in Electrical and Electronics Engineering
Supervisor: Assoc. Prof. Dr. Tolgay KARA
January 2021
65 Pages

In the last half century, especially industrial, robotic and automotive sectors started to take an important place in our lives with developing technology. The working principles of these sectors are mostly based on mechanical systems. One of the biggest factors that affects the working mechanism of a system negatively is the backlash formed in the mechanical parts. In order to reduce the damage caused by the backlash in mechanical systems, backlash must be compensated. The first stage of this starts with the identification of backlash size. Therefore, this thesis focuses on the identification of backlash size formed in mechanical systems. For this purpose, using computer simulation two feedback control system models, the first one for a mechanical system with backlash and the other one for a mechanical system without backlash, have been created. Kalman filter has been designed to see and understand the effect of backlash on load positions more accurately. Changes in load positions have been observed by using step input signal. Sum of the absolute value of the differences between load positions with backlash and load positions without backlash has been obtained. In order to achieve the value of estimated backlash size, an equation proportional to the obtained absolute sum result has been formulated. Estimated backlash values have been obtained by performing simulation experiments for different actual backlash values and their accuracy has been confirmed.

Key Words: Backlash, Gear, Kalman-Filter, Position Control, Backlash Identification

ÖZET

ELEKTROMEKANİK SİSTEMLERDEKİ MEKANİK BOŞLUĞUN KONTROL AMAÇLI TANILANMASI

ÇAKAR, Mehmet Fatih
Yüksek Lisans Tezi, Elektrik-Elektronik Mühendisliği Bölümü
Danışman: Doç. Dr. Tolgay KARA
Ocak 2021
65 Sayfa

Teknolojinin gelişmesiyle birlikte yaklaşık son yarım asırda özellikle endüstri, robotik ve otomotiv sektörleri hayatımızda önemli bir yer edinmeye başladı. Bu sektörlerin çalışma prensipleri daha çok mekanik sistemlere dayanmaktadır. Bir sistemin çalışma mekanizmasını olumsuz etkileyen en büyük faktörlerden bir tanesi mekanik aksamlarda oluşan boşluklardır. Mekanik sistemlerde oluşan boşluğun verdiği zararları azaltmak için boşluğun telafi edilmesi gerekmektedir. Bunun da ilk aşaması boşluk boyutunun tanılanmasıyla başlar. Bu nedenle, bu tez mekanik sistemlerde oluşan boşluk boyutunun tanılanması üzerine odaklanmıştır. Bu amaç doğrultusunda, bilgisayar simulasyonu kullanılarak mekanik sisteminde boşluk olan ve mekanik sisteminde boşluk olmayan geri beslemeli iki control sistemi oluşturuldu. Boşluğun yük pozisyonları üzerindeki etkisini daha doğru görebilmek ve anlayabilmek için Kalman filtresi tasarlandı. Adım giriş sinyali kullanılarak yükün pozisyonlarındaki değişiklikler gözlemlendi. Sistemde boşluk varken oluşan yük pozisyonları ile sistemde boşluk yokken oluşan yük pozisyonları arasındaki farkların toplamı mutlak olarak elde edildi. Boşluk boyutunun tahmini değerine ulaşabilmek için elde edilen mutlak toplam sonucuyla orantılı olarak bir denklem oluşturuldu. Mekanik sistemdeki farklı gerçek boşluk değerleri için simulasyon deneyleri yapılarak tahmini boşluk değerleri elde edilip, doğrulukları teyit edildi.

Anahtar Kelimeler: Boşluk, Dişli, Kalman-Filtresi, Pozisyon Kontrolü, Boşluğun Tanılanması

"To those who do not give up even under the most difficult conditions…"

ACKNOWLEDGEMENTS

I would like to thank my supervisor, Assoc. Prof. Dr. Tolgay KARA for his guidance and support throughout the study. I am thankful for his encouragement and motivation. I am glad for having the chance to work with him and to study under his excellent supervision.

I would like to express my love and gratitude to my family for their support, always best wishes. Special thanks go to my dearest, Leyla, for believing in my success more than I did, for convincing me that completing this thesis and for her everlasting support.

I am grateful to my skillful and capable colleagues Hüseyin KURT and Ömer Faruk AYDIN in İstanbul Aydın University for sharing their experience, vast knowledge, sincere friendship and helping me through this thesis study.

TABLE OF CONTENTS

Page

LIST OF TABLES

Page

LIST OF FIGURES

Page

LIST OF SYMBOLS

$\boldsymbol{\alpha}$	Half of the backlash gap size[*rad*]
$\boldsymbol{\theta_l}$	Load position [*rad*]
$\boldsymbol{\theta_m}$	Motor position [*rad*]
$\boldsymbol{\omega_l}$	Load angular speed [*rad/s*]
$\boldsymbol{\omega_m}$	Motor angular speed [*rad/s*]
$\boldsymbol{\tau}$	Time delay [*s*]
$\boldsymbol{A}$	System matrix
$\boldsymbol{b_l}$	Load friction coefficient [*Nms/rad*]
$\boldsymbol{b_m}$	Motor friction coefficient [*Nms/rad*]
$\boldsymbol{B, BF}$	Control matrix
$\boldsymbol{c}$	Internal shaft damping [*Nms/rad*]
$\boldsymbol{C, C_l, C_m}$	Measurement matrix
$\boldsymbol{D_l, D_m}$	Feed-through matrix
$\boldsymbol{i_f}$	Final gear ratio
$\boldsymbol{i, i_g}$	Gear ratio
$\boldsymbol{i_{g1}}$	Gear ratio in first gear
$\boldsymbol{i_t}$	Transmission gear ratio
$\boldsymbol{J_m}$	Motor inertia [kgm^2]
$\boldsymbol{J_l}$	Load inertia [kgm^2]
$\boldsymbol{k}$	Shaft stiffness [*Nm/rad*]
$\boldsymbol{K_r}$	Feedback controller gain
$\boldsymbol{K_{fl}}$	Filter gain for load position with backlash
$\boldsymbol{K_{flno}}$	Filter gain for load position without backlash
$\boldsymbol{K_{fm}}$	Filter gain for motor position with backlash
$\boldsymbol{K_{fmno}}$	Filter gain for motor position without backlash
$\boldsymbol{Q}$	State weighting matrix
$\boldsymbol{R}$	Control input weighting matrix

$\boldsymbol{T_m}$	Motor torque [Nm]
$\boldsymbol{T_l}$	Load torque [Nm]
$\boldsymbol{u}$	Control signal
$\boldsymbol{x}$	Reference state vector
$\boldsymbol{\hat{x}}$	State estimate
$\boldsymbol{y}$	Output vector

LIST OF ABBREVIATIONS

LQR	Linear Quadratic Regulator
LQE	Linear Quadratic Estimator
LQG	Linear Quadratic Gaussian
PD	Proportional Derivative
ABB	ASEA Brown Boveri
PRBS	Pseudo Random Binary Sequence
DOF	Degrees of Freedom
MRGIA	Modified Recursive General Identification Algorithm
MSE	Mean Square Error

CHAPTER I

INTRODUCTION

1.1 Motivation

The existence of backlash is one of the biggest problems in electromechanical control systems. The control of systems with backlash has been the subject study since 1940's and it is becoming more popular subject for investigating with developing technology [5]. Backlash makes the control system non-linear. Whenever backlash appears inside a system mechanism as presented in Figure 1.1, it brings other problems such as exciting oscillation, wearing out mechanical parts because of impulse caused by uncontrolled backlash traversal and generating audible noise. In addition, backlash is a vital problem especially in industry and automotive sectors. It is a big obstacle for their operating systems.

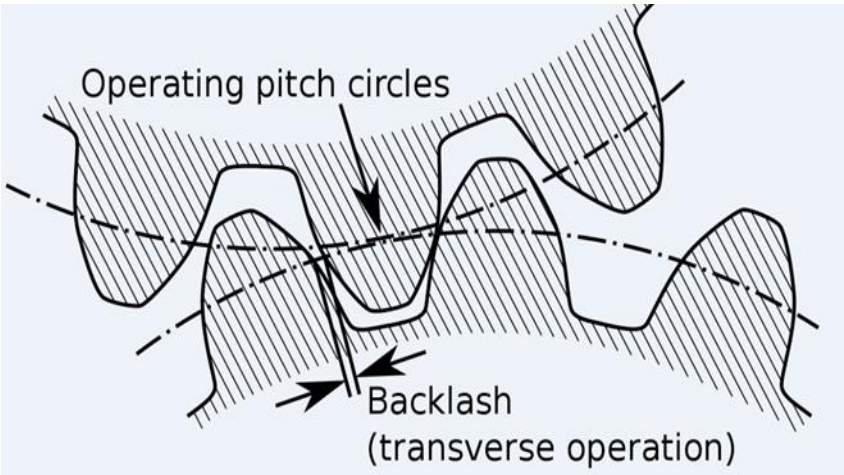

Figure 1.1 Backlash in mating gear transmissions

In order to get over all these problems mentioned above, the backlash size must be estimated before compensating backlash (see Figure 1.2). Therefore, this thesis focuses on the estimation of the backlash size. Simulation using the computer programs is the main solution to achieve the goal. Model based on comparing load positions which is one of the six parameters and using the difference between load

position with backlash and load position without backlash gives information about whether the backlash size is smaller or larger. Kalman-Filter (Linear Quadratic Estimator) is very important for observing load positions more accurately.

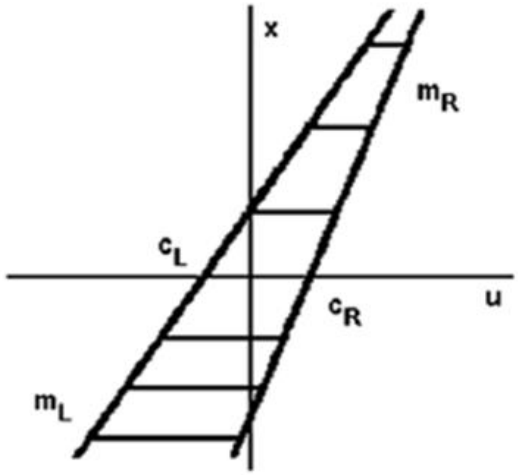

Figure 1.2 Backlash characteristic [4]

In this thesis study, mathematical model is proposed for backlash size estimation and it has been created according to the data coming from the sum of the absolute value of the difference between load position with backlash and load position without backlash. The estimated backlash values have been obtained for different actual values by using mathematical model. After obtaining estimated backlash values, percent error has been calculated by comparing it with actual backlash values. Simulation studies of backlash identification are included in this thesis. The results seem to be promising and thus the algorithm (simulation) should be working fine on backlash identification.

1.1 Literature Review

Lagerberg and Egardt [1] have developed nonlinear estimators of backlash size and status by using the principle of Kalman filtering. They have also defined a linear estimator for the rapid and precise estimate of the angular location of a wheel and motor. It uses normal motor speed sensors and the speed sensors of anti-lock brake system and event-based sampling of these sensors for each pulse. Lagerberg and Egardt [1] have tested the estimators by means of real-time vehicle and the findings

demonstrate that the calculations are of good quality and, thus useful in the powertrain control system to optimize the functions of backlash compensation [1].

Sainio [2] has studied on model-based calculation of backlash and successful compensation for the electrical powertrain in his work. The powertrain has been designed as a dual-mass mechanism with a rotating shaft. He combined the physical pattern of backlash with the model of two masses. In order to evaluate the size and location of backlash in the powertrain, two discretely time-shifted backlash estimators were built. Furthermore, for using in practice, he has developed an updated discrete-time backlash estimator. Sainio [2] has used grey-box design techniques to match the built-in powertrain model to the actual powertrain of the electric vehicle (Fiat Doblo). The calculation of the backlash size has been performed successfully. It has been found that the estimation of backlash location angle is strongly dependent on the precision of the powertrain model. In addition, two successful approaches for backlash compensation have been developed, tested and evaluated off-line. The first methodology of backlash compensation was based on the rule on custom regulation. It has been found that this is purely PD-controller. The Linear Quadratic Regulator (LQR) was the basis of second procedure. At the end of the study, it has been proved that the LQR method leads to precisely the same rule on motion control as the custom control legislation built [2].

Yang, Tang, Tan and Xu [3] have summarized five various detection methods on the basis of the dead-zone concept of backlash. Each development has been explicitly evaluated, primarily interpreting expectations, specifications for hardware and the issues that would be faced in reality. They confirmed the precision of theoretical study of different solutions by simulation measurements. By comparing these simulation results they obtained that the integral speed difference process, which involves few extra conditions and easy operation, can achieve reliable identification result only through a location sensor on the servo motor side. Therefore, they proved with experimental outcomes that it is very practical and the perfect identification method [3].

Vörös [4] has implemented a new analytical method of backlash characteristic definition, which uses relevant switching functions and their complements in his work. In the model equation, the backlash parameters have been separated from each

other; thus their estimation could be overcome as a quasi-linear problem using an iterative approach with internal estimation of variables. Vörös [4] has also provided the identification of cascaded structures consisting of an input backlash accompanied by a linear dynamic system. Simulation studies for the detection of backlash and cascaded structures are included in his study [4].

Nordin, Galic' and Gutman [5, 8] have extracted a modern, basic model based on phase-plane analytics for an elastic shaft with inner damping attached to a backlash. The model has been generalized to cover the case of so-called versatile coupling, in which rubber has filled part of the backlash space. Compared to simulations, extensive tests on an industrial drive with a compact binding matched very well. The classic dead-zone model provides an unphysical behavior of the dynamics with inner damping, but the new model which they obtained converged to standard dead-zone model as the damping happens to be zero [5, 8].

Haventon and Öberg [6] have applied the backlash estimating method as a control module in the ABB System Builder Prototype Library, for PLC programming a software program used in the ABB 800xA environment. They fulfilled industrial field measurements to verify the robustness of the procedure at the end of their study. The main purpose of their work is to expand the safety net to ensure that the robustness of the backlash identification method. The aim of the safety net in their study is to ensure that the estimation of backlash is only measured when the action of the mechanism approaches backlash [6].

Brunton and Kutz [7] have studied on inverted pendulum on the cart in chapter 8 of [7]. They applied a stabilizing controller to the system in order to consolidate the opinion of optimum control. The stability of open-loop system has been verified by checking the eigenvalues of system matrices. Then, they have checked the observability and controllability and designed full-state feedback (LQR), full-state estimation (Kalman Filter) and sensor-based feedback (LQG) solutions. These variables have been designed for both pendulum up fixed point and pendulum down fixed point. After completing these steps, for cost function, Brunton and Kutz [7] have defined Q and R matrices and then developed the LQR controller gain matrix.

They have simulated their system by using computer simulation program at the end of their study [7].

Lagerberg [9] has studied on control and estimation of powertrains in his another thesis. In the first part of his study, an outline of possible control techniques is given. He has divided the techniques into two categories as active and passive techniques, based on the way the controllers treats the backlash. Some of the techniques such as model predictive controllers and shifted linear controllers have been tested using simulation in the powertrain implementation. The findings of simulation have demonstrated that there is an ability of active non-linear controllers to enhance backlash control. Lagerberg [9] has used optimum open-loop control in his study as a means of identifying to determine theoretical limits for the efficiency of backlash compensation. In the second part of the thesis, he has been studied on backlash size and measurements of the current state of the powertrain in order to obtain controllers with high-performance for backlash compensation. Two non-linear estimators which one of them is for estimation of state and the other one for backlash size estimation have been designed based on the principle of Kalman Filtering. Experimental findings and results of simulation have indicated that resulting predictions are of good quality [9].

Jukic and Peric [10] have described three distinct methods to compensate the effect of backlash in the position-controlled mechanism. In the first method which is cascade structured position controller with an internal torque control loop, the effect of backlash have been compensated by the use of a powerful linear torque controller, at the cost of acquiring to calculate the shaft torque. They have defined the backlash model in method 2 as make it possible to compensate the effect of backlash by superimposing the compensation signal. This approach is, however, more susceptible to measuring noise. With input signal restrictions, in method 3 which is variable structure controller has been proved to be fine. Jukic and Peric [10] have selected these techniques since in the managed framework, they have considered most suitable in terms of computational and structural constraints. In a laboratory model, outstanding system actions have been experimentally tested while the suggested control principles have been used [10].

Acho, Ikhouane and Puja [11] have overcome the issue of regulation in the face of external disturbance by designing a strong feedback controller for backlash systems. The non-linear issue has been stated in the linear H_∞ framework by referring to the static dead-zone paradigm as a paradigm for backlash. They have performed an industrial simulation experiment with backlash and they have obtained an appropriate result [11].

Mola, Khayatian and Dehghani [12] have introduced a new technique for the detection and adaptive location control of two-mass mechanisms with rough non-linearity and undefined physical parameters of unknown backlash. Their identification procedure is formed of two cascade blocks. The first block is a linear system for parameters and the other one is an iterative method based on measuring of shaft's physical parameters. Based upon the Lyapunov principle, the dynamic controller has been designed in order to control the location of the load. The findings of simulation on the mechanism of two-mass model have demonstrated the efficacy of algorithms for detection and control [12].

Reyland. Jr. and Bai [13] have designed a method to identify the linear component of a block-oriented Wiener Model of the finite impulse response in their study. Non-linear block is the function of common backlash with non-linear decreasing and increasing functions. Just the crossing points of horizontal axis have been supposed to be known as a priori. They have suggested an algorithm for identifying and then developed identifiability. In addition, at the end of their study, the findings of the simulation experiment have been presented and debated [13].

Tarbouriech, Queinnec and Prieur [14] have discussed the topic of stability evaluation for linear construction in the loop with backlash and saturation. The resulting model which is a dynamic system with saturation and backlash has been regulated by static performance of feedback. Based on the stability properties of open-loop scheme, universal ultimate boundary stability has been discussed in global or local sense. They have defined appropriate regions of the state-space where orbits of closed-loop could be captured, along with estimations of the attracting basin of these regions. In order to provide a workable solution, they have suggested convex optimization issues [14].

Sarkar, Ellis and Moore [15] have set out the requirement as a first step of modeling for the usage of non-linear damping and elastic forces in the establishment of the gear-tooth reaction force. In the second step of modeling, a comprehensive multi-body simulation has been used to build and validate the efficacy of the proposed identification strategy. They have tested the validity of the technique by experiments. In the last stage, they have analyzed by the findings for testbed system and then it has demonstrated that their technique could be beneficial for observing the state of industrial mechanisms [15].

Barreiro and Banos [16] have aimed to research the reliability of systems with backlash, through an input-output perspective point in their work. In the first section, an overview of L_∞ has been discussed. This overview has presented criteria for the bounding of the loop signal and also helped for uniqueness and presence of solution by using Schauder fixed point principle. They have analyzed the system by utilizing the L_2 or the conical sector methodology in the second section. The graph of the backlash has been restricted to some conical field, which has been shown to be optimal. The conical inequality has triggered frequency conditions on the linear component, which have been further eased by the implementation of dynamic multipliers. In the last stage, both L_∞ and L_2 approaches have been merged in order to obtain a final requirement that results in a Popov-like state of stability [16].

Hovland, Hanssen, Moberg, Brogardh, Gunnarsson and Isaksson [17] have dealt with the problem of automated backlash detection in robot transmissions in their study. They have define a technique for identifying the backlash automatically by using the measurements of torque and location in the robot transmissions. Therefore, in automatic checks, only transmissions which have not met the backlash criteria needed to be tested and manually changed [17].

Yumrukçal [18] has aimed to implement the necessity for a dynamic system of a gear backlash in servo system that is to be utilized as a basis for controller creation. Throughout his thesis study, he has defined an actual servo mechanism with a gear backlash and a dynamic system of model has been created. In comparison of simulation findings with the test outcomes derived from physical system, the simulation findings for system model and the accuracy of the servo system with different backlash limitations have been addressed [18].

Lagerberg and Egardt [19] have defined non-linear estimation techniques for backlash location and size, all based upon principle of Kalman filtering in their another study. The estimators of location and size have been merged and the result has been an approximation of the backlash situation. This knowledge could be utilized in rotating mechanism's feedback control. Findings of simulation and experiments have demonstrated that predictions have been good quality and stable for modelling errors [19].

Tao and Kokotovic [20] have designed an adaptive control system for mechanisms with uncertain backlash at the output of the plant. A backlash reversed controller has ensured precise performance monitoring in the situation of a known backlash. Adaptive regulations have been developed to modify the parameters of the controller and to ensure the reliability of bounded input-output if the backlash parameters are uncertain. Simulations have demonstrated that these adaptive reversed controller had greatly improved the performance of the mechanism [20].

Tao and Kokotovic [21] have consolidated their recent findings in adaptive control of models with unidentified non-linearities including hysteresis, dead-zone and backlash parameters at the either input or output of linear modeling in their another study. Their adaptive reversed method has used an adaptive controller configuration composed of an adaptive reversed to eliminate the influence of an undefined non-linearity and a rule of an adaptive control for both defined or undefined linear dynamics. A linearly parameterized error mechanism has been designed for helping them to construct reliable adaptive rules to adjust the variables of the controller in order to guarantee boundedness of the closed-loop signal and enhance the efficiency of system monitoring ın spite of the bilinear dependency on the uncertain parameters [21].

Cerone, and Regruto [22] have introduced a two-stage method in their study in order to derive variables boundaries of linear structures including input backlash whenever the calculation errors of the output have been limited. Firstly, they have constrained closely the variables of the non-linear adaptive block by utilizing steady-state input and output information. After that, Cerone, and Regruto [22] have tested close bounds on the unquantifiable internal signal, that along with noisy output

calculations in order to restrict the variables of the linear adaptive model by giving an appropriate PRBS series [22].

Papageorgiou, Blanke, Niemann and Richter [23] have discussed the issue of measuring dead-zone width correctly in a singular axis mechanical powertrain system in their article. They have utilized a method containing a sliding mode monitor and a nonlinear dynamic optimization algorithm in order to evaluate the backlash size of dead-zone model between motor side and load side. The efficacy of the method has been showed by simulations [23].

Ruderman, Hoffmann and Bertrm [24] have provided a new method to the simulation and detection of flexible robot joints including backlash and hysteresis in their study. Their approach incorporates the dynamic responses of a rigid mechanical manipulator with flexible joints. The system involves electromechanical subsystems of gear and motor by which the relation between implemented torque and the joints torsion is known. The friction action of both patterns of pre-sliding and sliding has been incorporated by the Model of General Maxwell-Slip. Hysteresis has been defined by an operator of Preisach. The variables of dispersed model have been defined by using experimental data which collected from inner signal systems and the outer angular encoders installed to the second joint of the 6-DOF robotic system. The accuracy of the described model has been verified by its estimation agreement with separate experimental evidence not previously utilized to identify the model. The received model has provided a way for new sophisticated high precision robotic manipulator mechanics control [24].

Wang, Su and Hong [25] have addressed dynamic control of a group of continuous non-linear adaptive structures followed by an undefined dead-zone in their article. A stable dynamic control system has been built without creating a reversed dead-zone utilizing a new definition of the dead zone and trying to explore the features of this dead-zone template instinctively and mathematically. The new control strategy has guaranteed the global reliability of the dynamic system and obtained the desired monitoring accuracy. Simulations done on a standard non-linear model have explained and made clear the validity of their strategy [25].

Dong, Qıngyuan Tan and Yonghong Tan [26] have suggested a recursive approach for identifying output backlash structures which could be defined by using pseudo-Wiener model in their work. In this approach a new definition of the non-linear component of the system, i.e., backlash has been created. The non-linear model has been divided into a linear system which is piecewise in this situation. In order to determine the variables of the suggested model, a modified recursive general identification algorithm (MRGIA) then has been used. In addition, the integration of the MRGIA for the pseudo-Wiener method including backlash has been studied. A numerical illustration has been ultimately provided [26].

Cerone, Piga and Regruto [27] have introduced a method in order to derive parameter boundaries of linear systems including output backlash while output parameter errors have been limited. Firstly, the backlash parameters have been constrained by utilizing steady-state input and output information. After that, provided the expected unknown backlash and the output calculations gathered exciting the mechanism with a Pseudo-Random Binary Sequence (PRBS), boundaries have been measured on the unquantifiable internal signal. Ultimately, these boundaries, along with the input series, have been utilized to bind the parameters of linear block [27].

Dong and Tan [28] have suggested an on-line algorithm to define sandwich structures including backlash in their article. In this approach, backlash sandwich structures could be converted to a specific model in which all parameters of model have been divided based upon the so-called theory of main term segregation. In this situation, a piece-wise template has been achieved by linear coefficients coupling with non-linear parameters. And, for estimating the parameters of suggested system, an extended recursive recognition algorithm has been utilized. They have ultimately provided the consequences of the modeling on an X-Y placement stage [28].

In his another study, Vörös [29] has dealt with the simulation and recognition of non-linear cascade and sandwich structures with backlash in which general slopes have been taken into consideration, rather than straight lines defining the downward and upward portions of the backlash characteristics. This has made mechanical components' modeling more accurate and increased the efficiency of control

mechanisms. The analytical definition of the common backlash has contributed to mathematical model of the cascade mechanism including output common backlash and the sandwich mechanism including inner general backlash, in which all the parameters of the system have been segregated. Therefore, the identification has been resolved as a quasi-linear problem. Iterative methods have been suggested for approximation of internal parameters and illustrative instances have been included [29].

Lagerberg [30] has researched on backlash control in his another study and findings have been grouped into a specified format, in which major groups are active and passive non-linear and linear controllers. This research focuses on control methods appropriate for implementations in automotive powertrain, however the findings published are not restricted to this area. The findings reported are focused on partially distinct system models, based upon how the backlash integrated into the system. Various models of backlash have also been utilized. The study also includes a portion that explains these variations as well [30].

Ezal, Kokotovic, and Tao [31] have compensated a mechanism including flexibility and backlash by an optimum open-loop control rule coupled with the linear partial-state feedback rule. The backlash compensation has been viewed as optimally controlled rendezvous issue, whereas the linear flexibility controller has been developed utilizing classic control theory and single disturbance theory methods. Simulation findings have demonstrated substantial changes in the efficiency of system monitoring when backlash compensation has been active [31].

Hägglund [32] has introduced a new approach for the identification and measurement of backlash in control loops. The method for identification is based upon standard operational data. It is not presumed that output from the backlash has been calculated. His method is automated in in the sense which the user does not have to supply any input to operate the method. As the method provides an estimation of the dead-band induced by the backlash, the method provides all information necessary for compensating the backlash [32].

Grundelius and Angeli [33] have addressed two separate dynamic controllers which one of them in discrete time and the other one in continuous time for mechanisms including backlash operating on the input. Both systems have been based upon the linear controller and a reversed backlash. Uncertain parameters of the system and size of the backlash have been measured. The measured parameters have been utilized for controller's pole positioning design and for compensation of inverse backlash. Some researches of the estimator convergence have been performed. Simulations of the plant have demonstrated that both systems have good behavior [33].

Angeli [34] has introduced a variety of adaptive strategies in his work for compensating the backlash through a suitable feed-forward non-linear operation. Simulations results have demonstrated positive behavior for both explicit and implicit methods [34].

Merzouki, Davila, Fridman and Cadiou [35] have built second order sliding mode of limited time convergence for an electromechanical device including backlash in their article. As a result of the limited time integration, the sliding mode of control has been utilized to implement the recognition algorithms to describe the backlash phenomena. The magnitude of dead-zone and disturbing torque have been defined asymptotically. Experimental testing and simulation have been implemented to an electromechanical control module to help the theoretical development [35].

1.2 Objectives of the Thesis

The objective of this thesis has been set by simulation using computer programs. The main purposes are listed below:

- The major goal of this thesis is to identify the backlash size in electromechanical control systems for obtaining safety net to guarantee the reliability, functionality and robustness of operating conditions.
- Another purpose is to create more suitable environment for compensating of backlash and designing a control system in next stages.

- The other aim is to eliminate the effects of backlash which limit the performance of speed and position control in industrial, robotics, automotive and other applications by identifying backlash size.

1.3 Method

Before attempting to characterize and identify mechanical backlash, it is important to understand the effects of the backlash phenomenon on mechanical systems and position control problems. Therefore, in order to study on identification of backlash, the impacts of the backlash had to be understood first. At this point, simulation using the computer programs is very important to achieve the goals. Process for estimation of backlash has been investigated by starting to understand the idea of backlash. The method used in this thesis study has been extensively analyzed before passing the implementation of the work. It is basically depend on the computer programming language.

1.3.1 Computer Simulation Program

The basis of simulation studies in this thesis is software programing platform. Simulation could be defined as a graphical language of computer software program and it is designed by block diagrams. This block diagram language method can be used in a dynamic system for several purposes such as analysis, modeling and simulation of the system. Achieving these purposes is very easy in simulation program because the required components can be chosen from the library and these selected components can be also combined to each other by the way of block schedule. The library of computer simulation program includes a wide range of components which are available for insertion into the model. Luckily, the backlash block is one of these components. The backlash block as it is seen in Figure 1.3 has been used throughout this thesis study by adding it to the system.

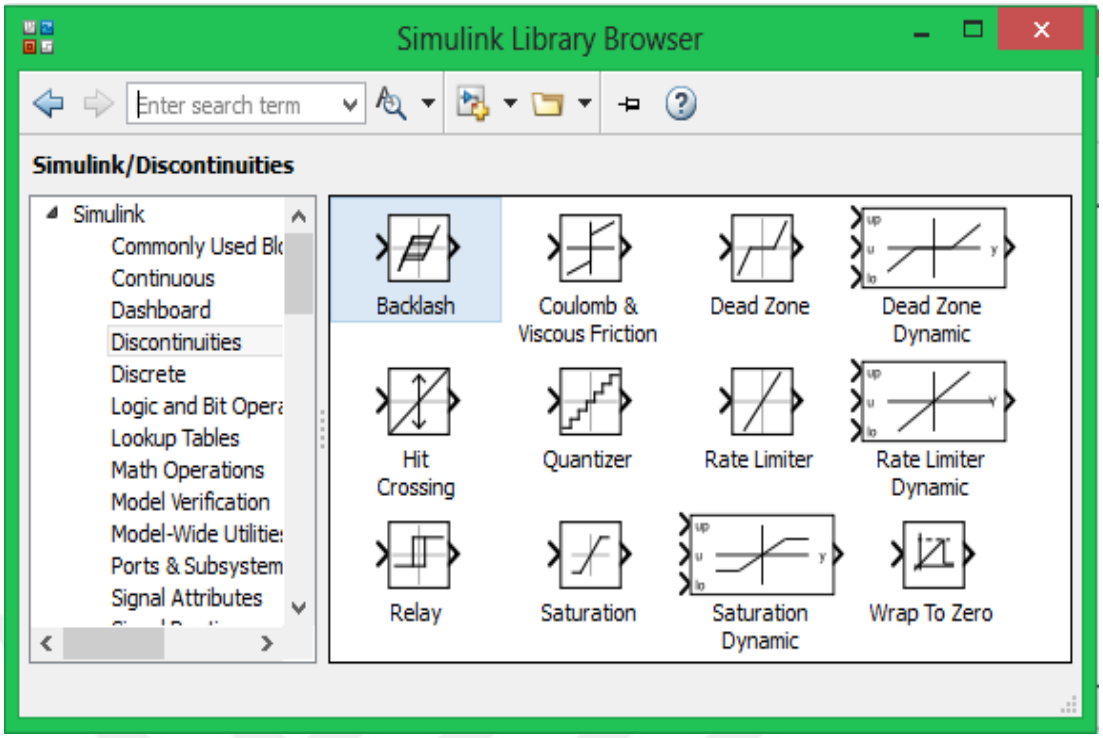

Figure 1.3 Backlash block in computer simulation program

As it is mentioned above the library of simulation program has wide range components to select. Various components of this library have been used in this thesis study. There are given the components used through the study with their purposes in Table 1.1.

Table 1.1 Various components of the library of computer simulation program used through this thesis study

	Step signal has been used as an input signal
	Backlash has been used as a disturbance in the system and it is the amount of the gap or play.
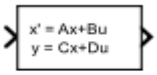	State-Space Model
	Band-Limited White Noise With Very Small Size (it has been chosen very small in order to observe backlash effect)
	Kalman-Filter has been used for observing measurements over time(load position used in this thesis study) to estimate unknown (backlash) parameter
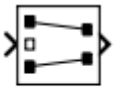	Selector has been used for observing load position change over time(there are six parameters)
	Linear Quadratic Regulator has been used as a feedback controller
	Scope has been used to see the variables on graph
	Mux which is also known data selector has been used for the purpose of forwarding several input signals to a single output line in some cases of this thesis study
	Function block has been used to calculate sum of the absolute value of the difference between load position with backlash and without backlash, in order to estimate backlash value and to obtain percent error estimation
	Constant has been used as actual backlash value in order to calculate percent error estimation
	Numeric display has been used to see some numerical values such as actual backlash size and estimated backlash size

Computer simulation program is not a real-time simulator [6]. It means that while the mechanism or system is operating, there will be no interaction with the mechanism because the time scale is altered. This creates generally a significant benefit since it is possible to implement a simulation of very long time in a short time like under ten seconds, although there could be some disadvantages for detection of backlash. However, the disadvantages are observed rarely.

1.4 Structure of the Thesis

Chapter II gives the general information about backlash system. Mathematical model of backlash is illustrated. There are the meanings of each symbol which are used through the thesis study. Simulation schematic of backlash identification is demonstrated. In addition, three backlash models which are vibration-impact backlash model, hysteresis model of backlash and dead-zone backlash model is described in this chapter.

Chapter III is related with parameter estimation. The matrices utilized in state-space model are introduced. The definitions of controllability and observability are given. The methods for determining whether the system is controllable or not controllable and whether the system is observable or not observable are explained. In this chapter, how to design the Linear Quadratic Regulator (LQR) for the system is defined. Then, augmented matrix is created and it is utilized for obtaining Kalman filter. This chapter also gives the information about the ways in order to achieve the LQR and Kalman filter design. The purposes of Kalman filter and LQR are explained here and there is shown a graph which has been obtained to understand the aim of Kalman filter.

In Chapter IV, simulation studies are given. Function block in computer programming platform is introduced here. After introducing Function block, estimated backlash size is obtained thanks to this block. There are some simulation graphs of estimated backlash sizes for several actual backlash sizes (these graphs have been obtained during the study). Comparison of estimated backlash size with actual backlash size and percent error estimation are shown in a table. The effect of backlash in the system is also can be seen on the graphs in this chapter.

Chapter V is related with the conclusion and recommendation of the thesis study and discusses the developments basis of the results. Some suggestions are given for future work in this chapter. What can be done after this thesis study and how to improve this study also mentioned in this chapter as a continuation.

In Appendix A, some examples which have been obtained from this thesis work are given. There is given a Curriculum Vitae (CV) and an article derived from the thesis at the end of this thesis study.

CHAPTER II

BACKLASH

There some significant non-linear effects that generally influence the control systems in the real world. Some of these effects are [34];

- Friction
- Time delay
- Backlash
- Saturation
- Un-modeled resonances
- Noise

Several approaches can be implemented to these effects. The simple approach is to ignore them. Another approach is that the effects could be included in the simulation model of the system. Then, the simulation must be run until making sure that the effects are negligible. If, contrarily, these effects result to in an important way the performances of the control system, there are some general measures that can be adopted, but the most appropriate remedies are usually tailored to the specific parasitics [34].

Backlash is a quantity of ‘‘play’’ or motion which is triggered by a gap between the components making contact with each other. The backlash is generally contained in mechanical systems. Actually, if the load side (driven side) is not connected to the motor side (driving side) directly, backlash can appear in all electromechanical systems like this (see Figure 2.1). Gear boxes, hydraulic valves and ball screw are the well-known examples [3]. When backlash exists in a mechanical system, it leads to the system being unreliable and uncontrollable. Therefore, backlash can seriously

restrict the efficiency of the control system. The motor side of the mechanical system has been assumed to be continuous (constant) component in this thesis study since the motor part is actuated by the step input signal. This input signal could be considered as a mass torque.

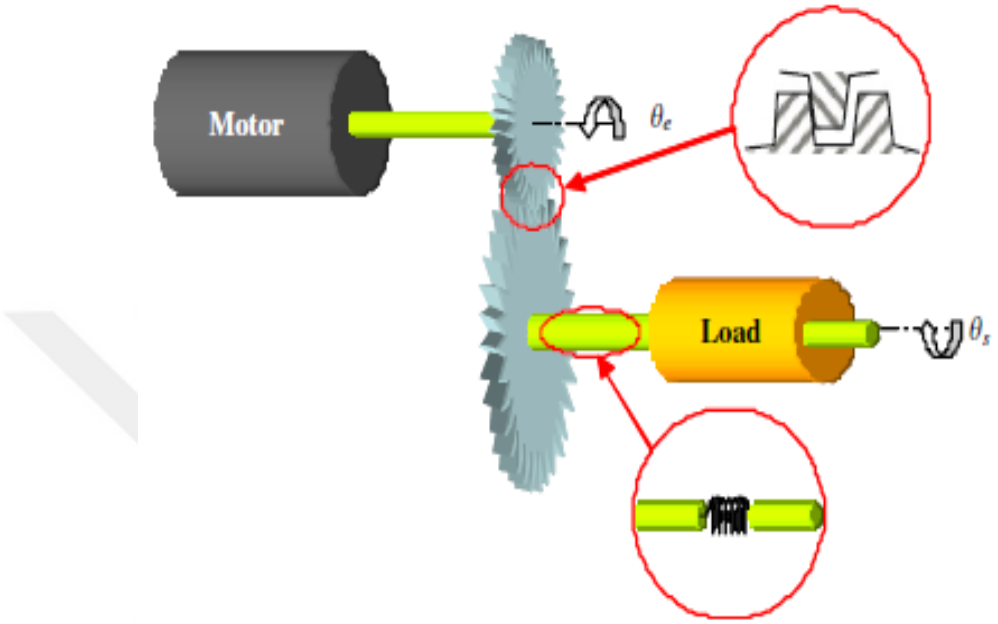

Figure 2.1 Connection of driving member (motor side) and driven member (load side) [35]

2.1 Sources of Backlash

There are several reasons of backlash. The important ones of these reasons will be mentioned. Poor lubrication of the system is one of the significant reasons for backlash. In order to obtain a well-built mechanism, the backlash should be reduced. However, there must be a sufficient amount of backlash between the moving components for enabling lubrication in order to protect the system against the deformation, stuck and high temperature. Hence, the presence of the backlash is usually a normal operating state for gears.

If the lubrication of the mechanism is not a good level or if the quality of the lubrication is poor, the rubbing of the components causes unwanted clearance that leads to adding backlash.

Figure 2.2 Backlash in mechanical system

Another reason of the backlash is related with manufacturing phase of the gears. Particularly, if the teeth of the gears are cut deeply at the beginning, it causes backlash. The other reason for increasing the backlash could be given as that tear and wear occurs as a result of backlash. This leads to larger backlash. Backlash also increases because of the age of the mechanism.

2.2 Mathematical Model of Backlash

In order to facilitate the description, a schematic diagram of backlash is shown in Figure 2.3 [3].

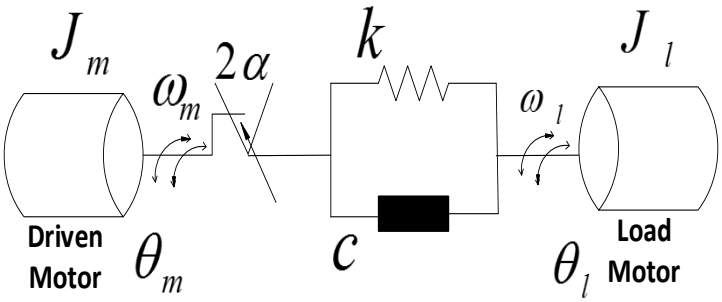

Figure 2.3 Schematic diagram of backlash

In Figure 2.3,

k is the shaft stiffness [*Nm/rad*]

c is the internal shaft damping [*Nm/(rad/s)*]

i is the total gear ratio (including final gear)

J_l is the load inertia [kgm^2]

J_m is the motor inertia [kgm^2]

b_l is the load viscose friction coefficient [*Nm/(rad/s)*]

b_m is the motor viscose friction coefficient [*Nm/(rad/s)*]

τ is time delay [*s*]

T_m is the motor torque [*Nm*]

T_l is the load torque [*Nm*]

θ_m is the output displacement (position) of the servo motor side [*rad*]

θ_l is the output displacement (position) of the load side [*rad*]

ω_m is the speed of motor side [*rad/s*]

ω_l is the speed of load side [*rad/s*]

α is the size of half of the backlash gap [*rad*]

The following numerical values for some symbols which mentioned above have been used through this thesis study.

$$\begin{cases} k = 3300 & Nm/rad \\ J_m = 0.4 & kgm^2 \\ J_l = 5.6 & kgm^2 \\ i = 3.984 & \\ c = 1 & Nms/rad \\ b_m = 0.1 & Nms/rad \\ b_l = 1 & Nms/rad \\ \tau = 1 & s \end{cases}$$

It is possible to obtain the gear ratio i as following [2]:

$$i = \frac{\omega_m}{\frac{\omega_l}{2}} \tag{2.1}$$

where ω_m is motor speed and ω_l is load speed. To give an example, let us say motor side has speed of 1000 rpm and load side has speed of 502 rpm. Then, the gear ratio will be:

$$i = \frac{1000}{\frac{502}{2}} = 3.984 \tag{2.2}$$

The obtained gear ratio value 3.984 has been used through this thesis study.

2.3 Backlash Models

In reality, backlash could exist in different locations of the transmission system. The non-linearity caused by backlash has various characteristics. When backlash appears, the torque is not moved from one side of the backlash gap to the other side of the backlash gap (input signal is assumed as torque in this study). The size of backlash gap is generally expressed by 2α size as shown in Figure 2.3. There exists a negative interaction when motor side and load side have an error of constant displacement (position) angle as the position angle of the motor side lags the load side by $-\alpha$. In this case, negative torque only could be implemented throughout the drivetrain system. On the other hand, when the position angle of the motor side leads the load side by α, there exists a positive interaction, and in this position, it permits merely positive torque to be implemented through the system. When the position angle of the motor side between α and $-\alpha$, interaction (contact) does not exist. Therefore, the torque is not moved to the other side. Several models of backlash have been analyzed. Backlash models which have been analyzed in this study are focused on these assumptions. All symbols used in models are in Figure 2.3 and the meanings of each symbol are written there.

2.3.1 Vibration-Impact Model

The problems related with this model contain two non-linear backlash mechanical models. One of these models is rigid impact model and the other one is elastic impact model. This model suggests that the affecting object is rigid, which means that the collision mechanism is instant, and it presents the coefficient of reflection in order to describe the energy lost in the impacting process. On the basis of the conservation of momentum, there are two equations [3] after impact as shown below. K is the coefficient of reflection here.

$$\dot{\theta_m}(t^+) - \dot{\theta_l}(t^+) = -K[\dot{\theta_m}(t^-) - \dot{\theta_l}(t^-)] \tag{2.3}$$

$$J_m\left[\dot{\theta_m}(t^+) - \dot{\theta_m}(t^-)\right] + J_l\left[\dot{\theta_m}(t^+) - \dot{\theta_l}(t^-)\right] = 0 \tag{2.4}$$

The calculations in this model are simple. Therefore, it makes the solutions analytically easier. This is the most important advantage of rigid impact model. However, this model neglects the relationship between phase and displacement, resulting in rigid impact method just matches the purely rigid frame.

Elastic impact model is another model of Vibration Impact problems. This model presumes that the impacting material is elastic. As the elastic features of this model could be linear, the features can be non-linear as well and duration of the collision mechanism is certain. The coefficient of variable stiffness is presented in elastic impact model on the basis of the errors in static transmission induced through manufacturing error and the dead-zone model.

The elastic impact model of the backlash is generally utilized in the dynamic study of the gear mechanism and this model is very complicated. Problems in the study of real control system are hard. They cannot be solved quickly. For this reason, elastic impact model is rarely utilized in the study of the driving control mechanism.

2.3.2 Hysteresis Model

The mathematical model for Hysteresis Backlash Model is mentioned below [3].

$$\omega_l = \begin{Bmatrix} \omega_m & \theta_l = \theta_m - \alpha \quad or \quad \theta_l = \theta_m + \alpha \\ 0 \end{Bmatrix} \tag{2.5}$$

If (2.5) is interpreted, it could be seen that the prediction of hysteresis backlash model is: The load side is constant while the motor side of the system is in the backlash zone. It could be split into two situations. The first case is that the load side is stationary when the motor side goes through to the backlash because of large damping. Backlash between the transmitting mechanism and the table of the system is an example of this situation. The other case is that the damping of the motor side and inertia moment is comparatively small. Therefore, the motor side can rapidly splash over the backlash for contacting with load side. The load side could be considered as stationary in this situation. The hysteresis backlash model is rarely utilized since the prediction of this model cannot be fulfilled in the most applications.

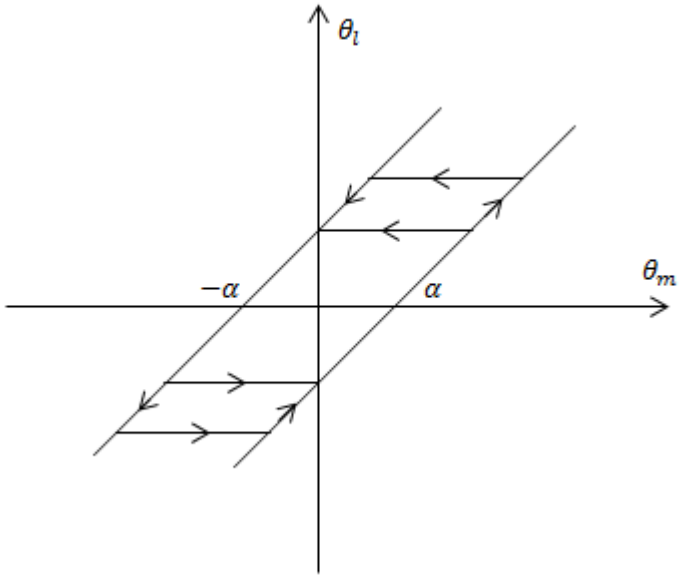

Figure 2.4 Hysteresis model of backlash

2.3.3 Dead-Zone Model

The representation of Dead-zone Backlash Model [3] mathematically is as follows. M_F is torque and $\Delta\theta = \theta_m - \theta_l$ here.

$$M_F = \begin{Bmatrix} k(\Delta\theta - \alpha) + c(\dot{\theta_m} - \dot{\theta_l}) & for & \Delta\theta > \alpha \\ 0 & for & -\alpha \leq \Delta\theta \leq \alpha \\ k(\Delta\theta + \alpha) + c(\dot{\theta_m} + \dot{\theta_l}) & for & \Delta\theta < -\alpha \end{Bmatrix} \quad (2.6)$$

Backlash between the transmission torque of the motor side and the load side of the mechanism is defined by the non-linear dead-zone model. Relative displacement $\Delta\theta$

is used as input and M_F which is torque is used as output in this model. The dead-zone model of backlash represents the relationship of the motor side and the load side with torque transfer and the model also takes into account the effect of the damping and stiffness of the mechanism.

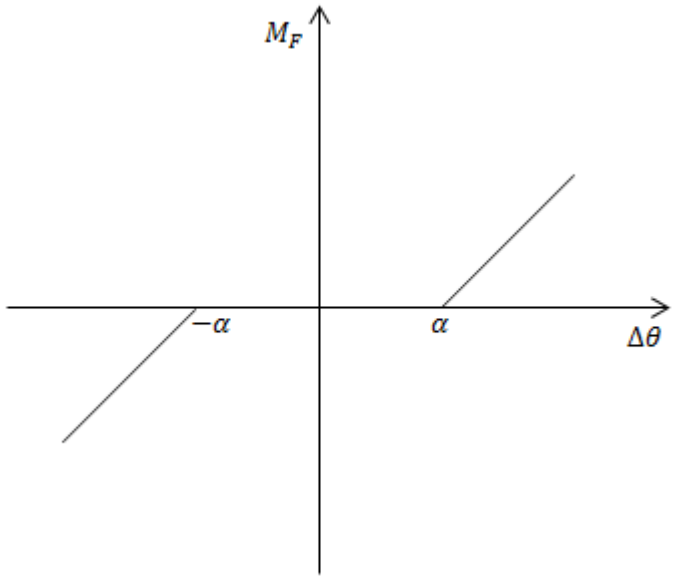

Figure 2.5 Dead-zone model of backlash

The concept of the Dead-zone Backlash Model is more practical in real servo systems since the entity surrounding backlash has two spinning inertias. Such a mechanism or system is closer to the real case of the backlash non-linearity and the research of non-linear backlash has more realistic importance.

2.4 Simulation Schematic of Backlash Identification

Input signal is step input signal in this study. Kalman filter has been used for observing load positions with backlash and without backlash more accurately. Selector has been used to choose load position parameter which is one of the six measurements of the system. LQR is a feedback controller here. Band-Limited-Noise is ignored (very small) to see the effect of backlash on the load position.

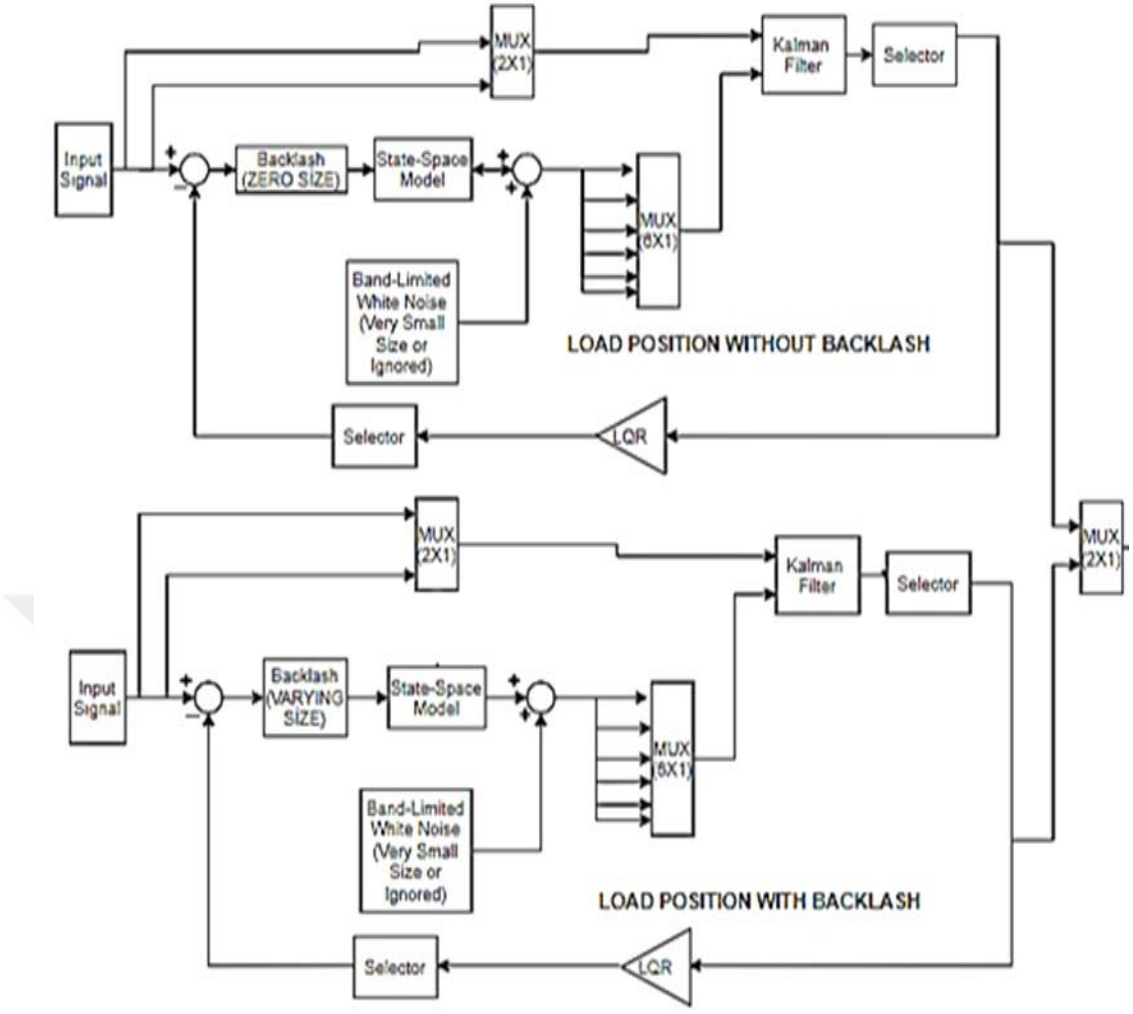

Figure 2.6 Block diagram of simulation system

CHAPTER III

PARAMETER ESTIMATION

The given system dynamics can be expressed in state-space form for using estimation of backlash parameters [1-2].

$$\dot{x} = Ax + Bu \tag{3.1}$$

$$y = Cx + Du \tag{3.2}$$

Where u is the requested motor torque and the state vector has six parameters as follows:

$$x = [\theta_m \quad \omega_m \quad \theta_l \quad \omega_l \quad T_l \quad T_m]^T \tag{3.3}$$

Where the six states of this state vector are;

- $x1 =$ motor position (displacement)
- $x2 =$ speed of motor side
- $x3 =$ load position(displacement)
- $x4 =$ speed of load side
- $x5 =$ load torque
- $x6 =$ motor torque

The measurement vector has motor position and load position parameters as follows:

$$y = [\theta_m \quad \theta_l]^T \tag{3.4}$$

According to system dynamics, the state-space has *A* and *B* matrices as

$$A=\begin{bmatrix} 0 & 1 & 0 & 0 & 0 & 0 \\ \frac{-k}{J_m i^2} & -\frac{i^2 c+b_m}{J_m} & \frac{k}{J_m i} & \frac{c}{J_m i} & 0 & \frac{1}{J_m} \\ 0 & 0 & 0 & 1 & 0 & 0 \\ \frac{k}{J_l i} & \frac{c}{J_l i} & -\frac{k}{J_l} & -\frac{c+b_l}{J_l} & -\frac{1}{J_L} & 0 \\ 0 & 0 & 0 & 0 & 0 & 0 \\ 0 & 0 & 0 & 0 & 0 & -\frac{1}{\tau} \end{bmatrix} \tag{3.5}$$

$$B=\begin{bmatrix} 0 & 0 & 0 & 0 & 0 & -\frac{1}{\tau} \end{bmatrix}^T \tag{3.6}$$

And the matrices of C and D are as the following:

$$C=\begin{bmatrix} 1 & 0 & 1 & 0 & 0 & 0 \end{bmatrix} \tag{3.7}$$

The motor position and the load position are measurable and *C* matrix takes the form separately

$$C_m=\begin{bmatrix} 1 & 0 & 0 & 0 & 0 & 0 \end{bmatrix} \tag{3.8}$$

for motor position and

$$C_l=\begin{bmatrix} 0 & 0 & 1 & 0 & 0 & 0 \end{bmatrix} \tag{3.9}$$

for load position. Then, the *D* matrix takes the form of

$$D=\begin{bmatrix} 0 \\ 0 \end{bmatrix} \tag{3.10}$$

3.1 Controllability and Observability

In linear control theory, the degree of closed-loop feedback $u = -Kx$ for controlling system's behavior in equation (3.1) should be known. The eigenvalues of unstable backlash system could be modified through closed-loop feedback, leading to a new system matrix $(A - BK)$ containing stable eigenvalues. This part offers precise conditions for when and how the dynamics of the system could be controlled via feedback.

3.1.1 Controllability

The capability of constructing the closed-loop system's eigenvalues through the selection of K depends on the controllability of the system in equation (3.1). In order to determine the controllability of a linear structure, the column space of the controllability matrix $\mathbf{C}$ is used.

$$\mathbf{C} = \begin{bmatrix} B & AB & A^2B & \dots & A^{n-1}B \end{bmatrix} \tag{3.11}$$

If the matrix $\mathbf{C}$ has n linearly independent columns, then the system in equation (3.1) is controllable [7]. In addition, the controllability of matrix $\mathbf{C}$ determines which state vector directions could be manipulated by control.

In computer programming language, the controllability of matrix $\mathbf{C}$ can be obtained by

$\gg ctrb(A, B)$.

And then it is possible to check the rank of the matrix in order to see whether it is equal to n or not, by using

$\gg rank(ctrb(A, B))$.

The controllability of the system has been checked and it has been obtained in computer programming language as in Figure 3.1.

```
>> ctrb(A,B)

ans =

   1.0e+06 *

         0         0    0.0000   -0.0000   -0.0012    0.0161
         0    0.0000   -0.0000   -0.0012    0.0161    1.2942
         0         0         0    0.0000    0.0004   -0.0027
         0         0    0.0000    0.0004   -0.0027   -0.3933
         0         0         0         0         0         0
    0.0000   -0.0000    0.0000   -0.0000    0.0000   -0.0000
```

Figure 3.1 Controllability of the system

3.1.2 Observability

The system's observability in equations (3.1) and (3.2) is almost similar to the controllability of the system mathematically. However the physical understanding varies slightly. If any state can be determined from the time history of the $y(t)$ parameters, this mechanism is observable. In order to determine the observability of the mechanism, completely the row space of the $\boldsymbol{O}$ matrix which is observability matrix of the system is used.

$$\mathbf{O} = \begin{bmatrix} C \\ CA \\ CA^2 \\ \vdots \\ \vdots \\ CA^{n-1} \end{bmatrix} \tag{3.12}$$

In computer programming language, the observability of matrix $\boldsymbol{O}$ can be obtained by

$\gg obsv(A, C)$.

The behavior of a controllable mechanism can be changed, but if there are no full-state parameters of x, we have to estimate x from the parameters. This can be achieved if the system is observable. If the mechanism is observable, the eigenvalues of the adaptive estimator system could be constructed with favorable features, such as efficient noise attenuation and quick estimation.

It is important to note that the observability criteria is the dual criteria of the controllability mathematically. The transpose of controllability matrix is equal to the observability matrix (A^T, C^T) and it is achieved in computer programing language by using

$\gg \boldsymbol{O} = ctrb(A', C')'$.

In this thesis study, variable of C in observability matrix has taken as C_m for motor side and it has taken as C_l for load side. It has been seen that the constructed state-space model is controllable and observable.

The observability of the system has been checked and it has been obtained in computer programming platform as in Figure 3.2.

```
>> obsv(A,C)

ans =

   1.0e+07 *

    0.0000         0    0.0000         0         0         0
         0    0.0000         0    0.0000         0         0
   -0.0000   -0.0000    0.0001    0.0000   -0.0000    0.0000
    0.0003   -0.0000   -0.0012    0.0001   -0.0000   -0.0000
    0.0395    0.0005   -0.1573   -0.0013   -0.0000   -0.0001
   -0.4476    0.0366    1.7832   -0.1566    0.0002    0.0013
```

Figure 3.2 Observability of the system

3.2 Linear Quadratic Regulator (LQR)

A significant objective of optimal control is choosing the right gain matrix K in (3.13) to balance the system without spending too much effort for control. The stability control law is given below.

$$u = -Kx \tag{3.13}$$

The expenditure of control must be taken into account in order to

- avoid over-reacting of controller to disturbances and high-frequency noise
- then, by doing this, the actuation does not surpass the permitted maximum amplitudes
- and so that control is not extremely costly

Especially, the cost function [7] which is given below has a great importance to balance the cost of state's efficient regulation with the cost of control.

$$J(t) = \int_0^t x(\tau)^* Qx(\tau) + u(\tau)^* Ru(\tau) d\tau \tag{3.14}$$

Respectively, the Q matrix is a measure of the cost of the state's deviations from zero and matrix R is a measure of the cost of actuation. These both matrices are always diagonal and the diagonal components can be modified to adjust the relative value of the control goals. Q is a semi-definite positive matrix and R is a definite positive matrix. The Q matrix has been set as follows:

$Q = eye(6)$.

In other words,

$$Q = \begin{bmatrix} 1 & 0 & 0 & 0 & 0 & 0 \\ 0 & 1 & 0 & 0 & 0 & 0 \\ 0 & 0 & 1 & 0 & 0 & 0 \\ 0 & 0 & 0 & 1 & 0 & 0 \\ 0 & 0 & 0 & 0 & 1 & 0 \\ 0 & 0 & 0 & 0 & 0 & 1 \end{bmatrix} \tag{3.15}$$

And the R matrix has been set as follows:

$$R = 0.0001 \tag{3.16}$$

The values of Q and R which are mentioned above have been used through this thesis study. The control low of LQR is similar to the stability control law as seen in (3.17).

$$u = K_r x \tag{3.17}$$

This law is utilized to minimize $J = \lim_{t\to\infty} J(t)$. Since it is a linear control rule developed for a linear system in order to minimize the quadratic cost function, LQR is so called and this regulates the system's state as $\lim_{t\to\infty} x(t) = 0$.

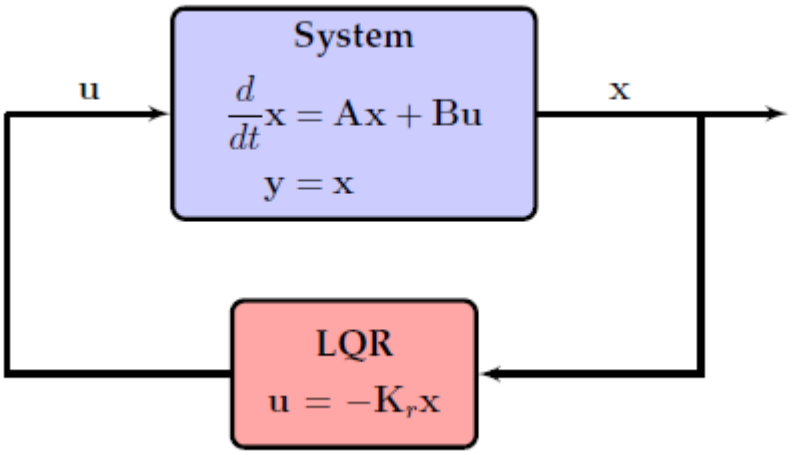

Figure 3.3 Schematic of the LQR for optimal full-state feedback [7]

K_r is a constant gain and it could be achieved by using several methods, but in this thesis there are two important methods. The first way is solving the Riccati algebraic equation [7].

$$K_r = R^{-1}B^*X\ , \tag{3.18}$$

X is the solution of the algebraic Riccati equation here.

$$A^*X + XA - XBR^{-1}B^*X + Q = 0 \tag{3.19}$$

By solving the Riccati equation in (3.19), X is obtained, so that constant gain matrix K_r is obtained. Another method for achieving constant gain K_r which has been used in this thesis is computer programming language. K_r has been used as K in this thesis study. It has been obtained via

$$\gg K = (lqr(A', C', Q, R))'\ .$$

LQR has been used as a feedback controller in this thesis study. The gain matrix K for optimal system has been obtained in computer programming platform as in Figure 3.4.

```
>> K

K =

   1.0e+03 *

    0.0758
    4.4009
    0.0868
   -1.1837
   -0.1000
    0.0106
```

Figure 3.4 Gain matrix K for optimal control

3.3 The Kalman Filter

Kalman filtering which is also known as linear quadratic estimation (LQE) is used for observing measurements of a mechanical system such as inaccuracies, statistical noise and backlash over time. Since the conflicting effects of these measurements are optimally balanced by Kalman filter, it is the most widely utilized estimator of full-

state. The state could be estimated from restricted noisy measurements of y, rather than measuring full-state of x. Actually, estimation of full-state is possible mathematically if the pair of (A, C) are observable.

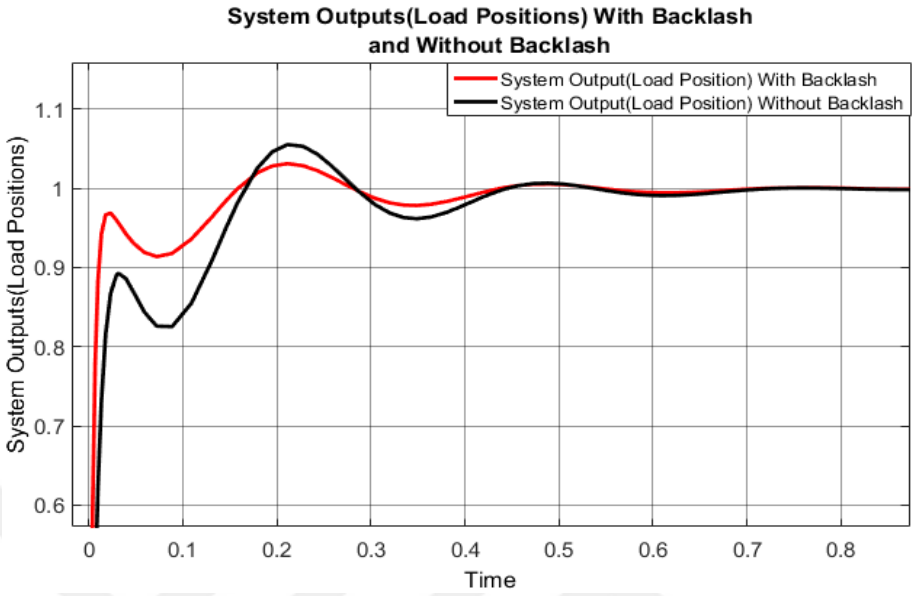

Figure 3.5 Observation of load positions by using Kalman filter: Black line: Load position with backlash, Red line: Load position without backlash

In this paper, Kalman filter has been used for observing load position (one of the six parameters) with backlash and load position without backlash more accurate. This is the main way to see the changes of load positions to create an idea for mathematical model. There is an example in Figure 3.5 which is taken from the simulation results. In this graph, red line shows the change of load position over time when there is no backlash in the system. On the other hand, the black line shows the change of the load position over time. The difference between the systems when there is backlash and when there is no backlash can be seen in this figure. The observation of the backlash effect has been obtained thanks to using Kalman filter.

Full-state estimate might be obtained by using Kalman filter with LQR feedback law which is optimal rule for estimation. Augmented system with backlash (disturbance) and noise (ignored or very small) as shown in Figure 3.6 has been re-arranged for deriving full-state estimator.

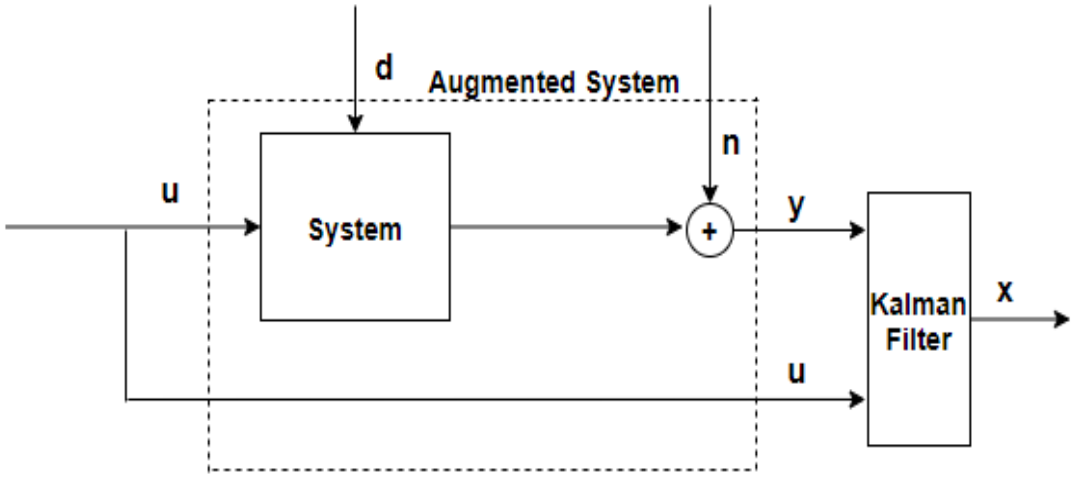

Figure 3.6 Augmented system with disturbance (backlash) and noise

Throughout the study, noise has been neglected in order to observe the effect of backlash (disturbance). Therefore, noise has been taken approximately zero in all equations.

$$\dot{x} = Ax + Bu + V_d d + 0n \tag{3.20}$$

$$y = Cx + Du + 0d + V_n n \tag{3.21}$$

V_d is disturbance (backlash) covariance matrix and V_n is measurement noise covariance matrix here. V_d and V_n are positive semi-definite matrices. A, B, C and D matrices have been obtained from system model. Random numbers have been created and they have been supposed to actual backlash size. V_n has been ignored for all cases. V_d measurement has been constructed for system with backlash as;

$V_d = randnumber * eye(6)$.

And V_d has been constructed approximately zero for system without backlash as;

$V_d = 0.00000001 * eye(6)$.

Augmented inputs with disturbance (backlash) and noise has been developed as below.

$BF = [B \;\; V_d \;\; 0 * B]$

```
>> BF

BF =

         0    4.4875         0         0         0         0         0         0
         0         0    4.4875         0         0         0         0         0
         0         0         0    4.4875         0         0         0         0
         0         0         0         0    4.4875         0         0         0
         0         0         0         0         0    4.4875         0         0
    1.0000         0         0         0         0         0    4.4875         0
```

Figure 3.7 Augmented inputs with disturbence (backlash) and noise

There are again several methods for obtaining the filter gain K_f, but two important similar procedures as in LQR will be explained. K_f can be obtained by using the first procedure which is solving Riccati equation and the other one is using computer program language. In the first method, the estimation $\hat{x}$ of the full-state x can be derived from input u and output y measurements by using dynamic system estimator which is shown below [7].

$$\frac{d}{dt}\hat{x} = A\hat{x} + Bu + K_f(y - \hat{y}) \tag{3.22}$$

$$\hat{y} = C\hat{x} + Du \tag{3.23}$$

and K_f is given by

$$K_f = YC^*V_n \tag{3.24}$$

y gives the solution of Riccati algebraic equation in (3.25).

$$YA^* + AY - YC^*V_n^{-1}CY + V_d = 0 \tag{3.25}$$

The Kalman filter is generally referred to as this approach. The other procedure is computer software language. The filter gain K_f has been defined for load position with backlash in computer programming platform as K_{fl} and it has been obtained via

$\gg K_{fl} = (lqr(A', C_l', V_d, V_n))'$.

```
>> Kfl

Kfl =

   13.6596
 -462.0474
  214.2064
  504.4727
 -211.8382
   22.2970
```

Figure 3.8 Filter gain for load position with backlash

For load position without backlash, it has been defined as K_{flno} and it has been obtained via

$\gg K_{flno} = (lqr(A', C_l', V_{dno}, V_{nno}))'$.

```
>> Kflno

Kflno =

    8.1290
  372.3904
  100.6749
   67.7136
 -100.0000
   10.4449
```

Figure 3.9 Filter gain for load position without backlash

As observability and controllability are mathematically dual problems, optimal estimation and control are also dual problems. Therefore, the filter gain for load position with backlash, K_{fl} might be obtained by using LQE as:

$\gg K_{fl} = lqe(A, V_d, C_l, V_d, V_n)$.

And the filter gain for load position without backlash, K_{flno} might be obtained by using LQE as:

$\gg K_{flno} = lqe(A, V_d, C_l, V_{dno}, V_{nno})$.

The results of the parameters which are state-space system with backlash and noise ($sysCl$), state-space system with backlash ($sysKFL$) and without backlash ($sysKFLNO$) are given in Appendix A. These results have been achieved during the thesis study.

CHAPTER IV

SIMULATION STUDIES

A simulation program which is a graphical language based on a computer programming platform [6] has been used in this study. This computer program has a wide library and fortunately, backlash block is a component of this library. Backlash block has been used through the article. By using this block, change of system output (load position) with backlash and without backlash have been observed. Estimations of backlash size have been tested in computer programing language and recorded for several values of actual backlash sizes. The performance of simulation studies is illustrated in the following examples. In the examples of ‘‘System Outputs (Load Positions) With Backlash and Without Backlash’’, x coordinate of these graphs represents ‘‘Time’’ and y coordinate of these graphs represents ‘‘System Outputs (Load Positions)’’. In the examples of ‘‘Comparison of Estimated Backlash Value with Actual Backlash Value’’, x coordinate of these graphs represents ‘‘Time’’ and y coordinate of these graphs represents ‘‘Actual Backlash Value and Estimated Backlash Value’’. Simulation tests have been applied for a duration of 2 seconds each.

4.1 Function Block and Backlash Size Identification

Function block allows us to use the computer programming platform for identifying custom functionality in the models of simulation. By using function block, the programming codes can be brought easily into the simulation part of the computer program. When a model which includes function block is simulated, these codes are integrated with the model. This block is used to study on identifying the class, complexity and size of the variables.

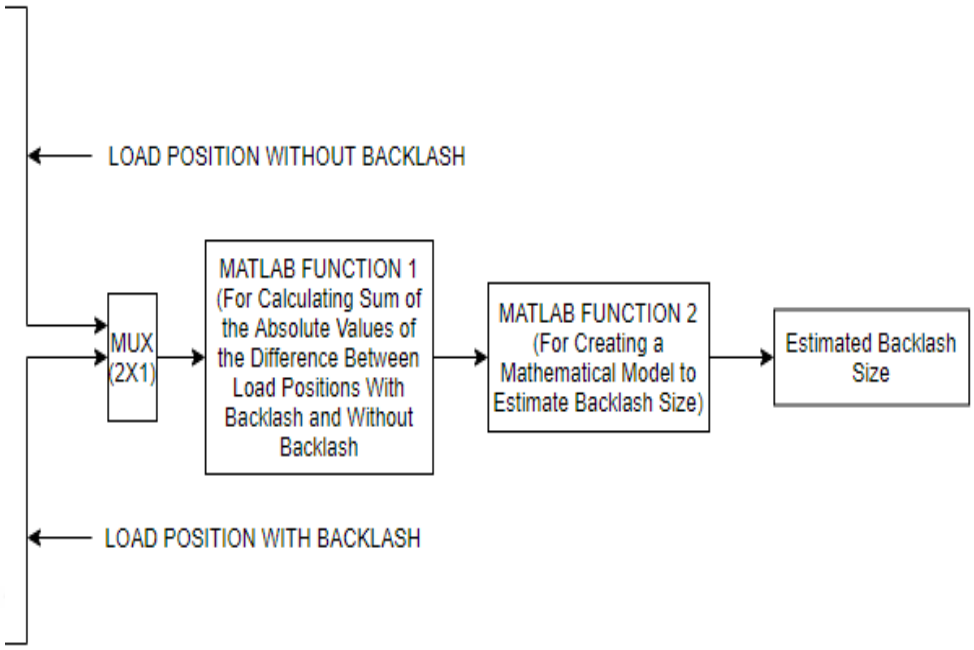

Figure 4.1 Function block in computer simulation

In order to get sum of the absolute value of the difference between load positions with backlash and load positions without backlash and to create an equation based on this sum for identifying backlash size, function block (see Figure 4.1) has been used.

Example 1. System output (load position) with backlash and without backlash is shown in Figure 4.2. Sum of the absolute value of the difference between load positions have been calculated as 3.624×10^{-4}. By using this result, the estimated backlash size has been simulated on the basis of actual backlash size which is 1.2234 (see Figure 4.3) and Band-Limited Noise with zero mean. Estimated backlash size has been identified as 1.183. The difference between actual backlash size and estimated backlash size is 0.0404.

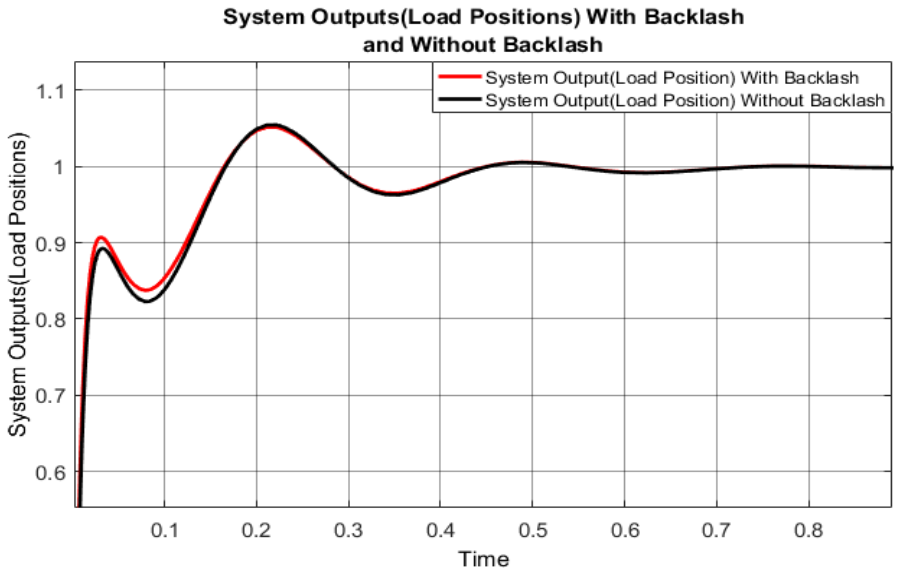

Figure 4.2 System outputs **(**load positions) change: Black line: Load position with backlash, Red line: Load position without backlash – Example.1

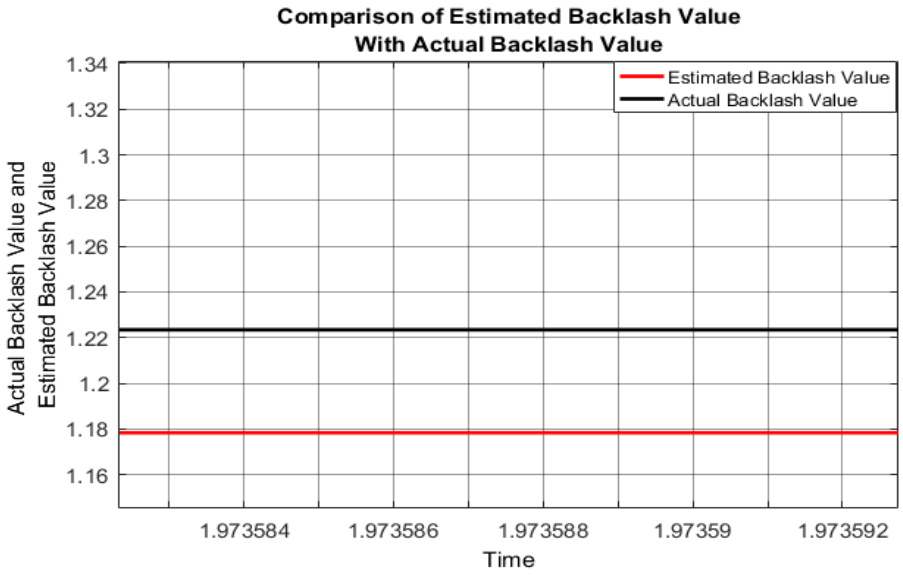

Figure 4.3 Actual backlash size and estimated backlash size: Black line: Actual backlash size, Red line: Estimated backlash size – Example.1

Example 2. System output (load position) with backlash and without backlash is shown in Figure 4.4. Sum of the absolute value of the difference between load positions have been calculated as 8.781×10^{-4}. By using this result, the estimated backlash size has been simulated on the basis of actual backlash size which is 1.7309 (see Figure 4.5) and Band-Limited Noise with zero mean. Estimated backlash size has been identified as 1.636. The difference between actual backlash size and estimated backlash size is 0.0949.

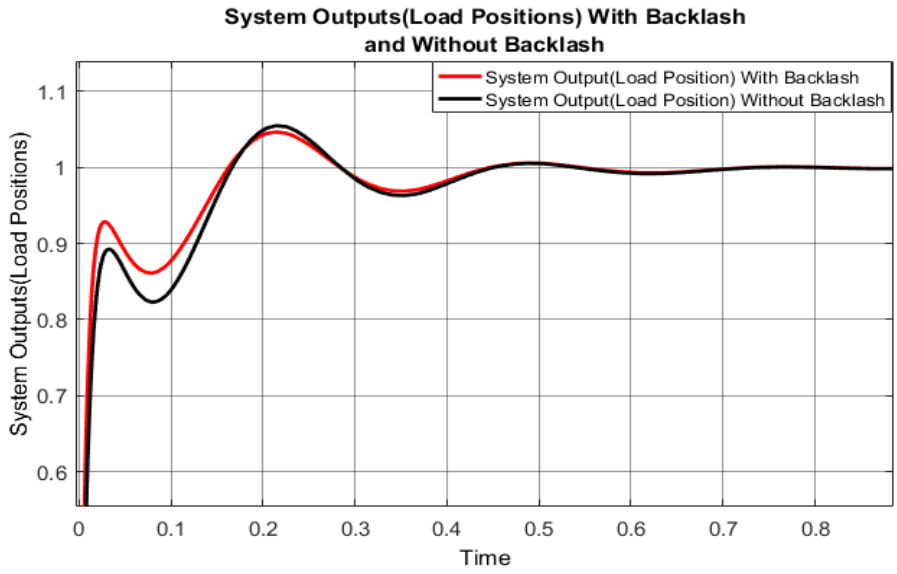

Figure 4.4 System outputs **(**load positions) change: Black line: Load position with backlash, Red line: Load position without backlash – Example.2

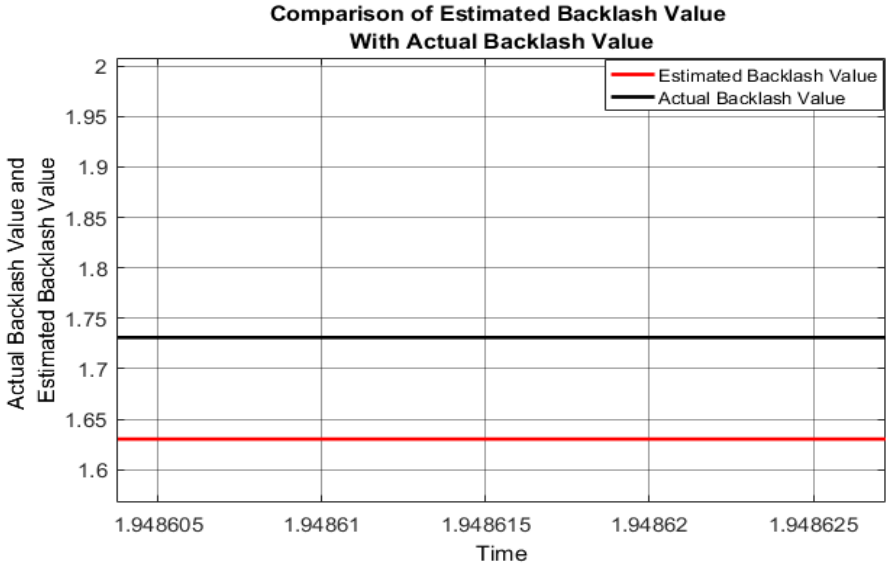

Figure 4.5 Actual backlash size and estimated backlash size: Black line: Actual backlash size, Red line: Estimated backlash size – Example.2

Example 3. System output (load position) with backlash and without backlash is shown in Figure 4.6. Sum of the absolute value of the difference between load positions have been calculated as 1.287×10^{-3}. By using this result, the estimated backlash size has been simulated on the basis of actual backlash size which is 2.3923 (see Figure 4.7) and Band-Limited Noise with zero mean. Estimated backlash size has been identified as 2.354. The difference between actual backlash size and estimated backlash size is 0.0383.

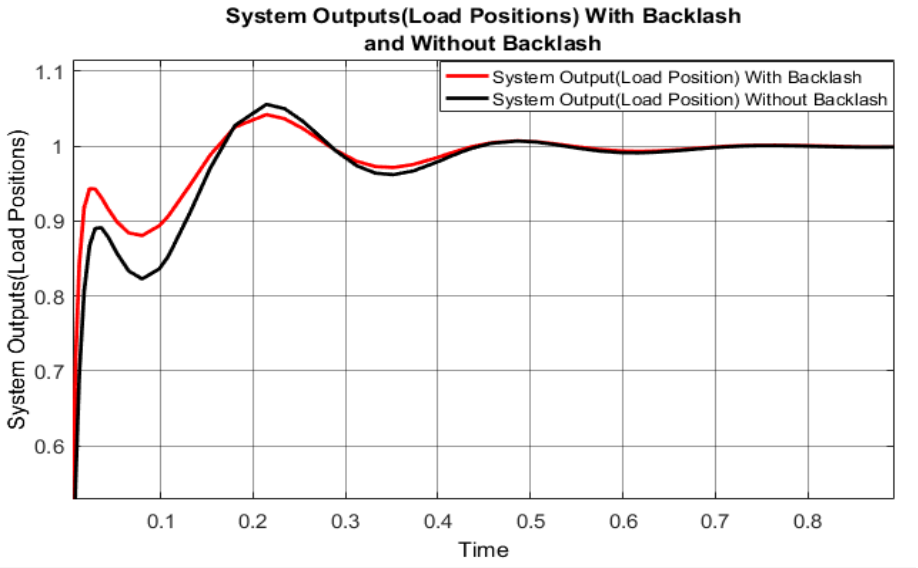

Figure 4.6 System outputs **(**load positions) change: Black line: Load position with backlash, Red line: Load position without backlash – Example.3

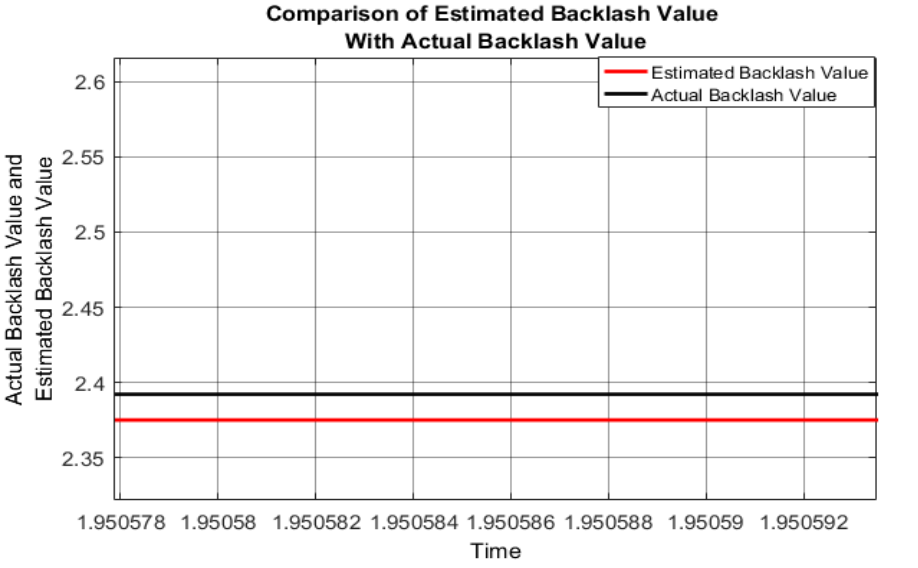

Figure 4.7 Actual backlash size and estimated backlash size: Black line: Actual backlash size, Red line: Estimated backlash size – Example.3

Example 4. System output (load position) with backlash and without backlash is shown in Figure 4.8. Sum of the absolute value of the difference between load positions have been calculated as 1.41×10^{-3}. By using this result, the estimated backlash size has been simulated on the basis of actual backlash size which is 2.5718 (see Figure 4.9) and Band-Limited Noise with zero mean. Estimated backlash size has been identified as 2.662. The difference between actual backlash size and estimated backlash size is 0.0902.

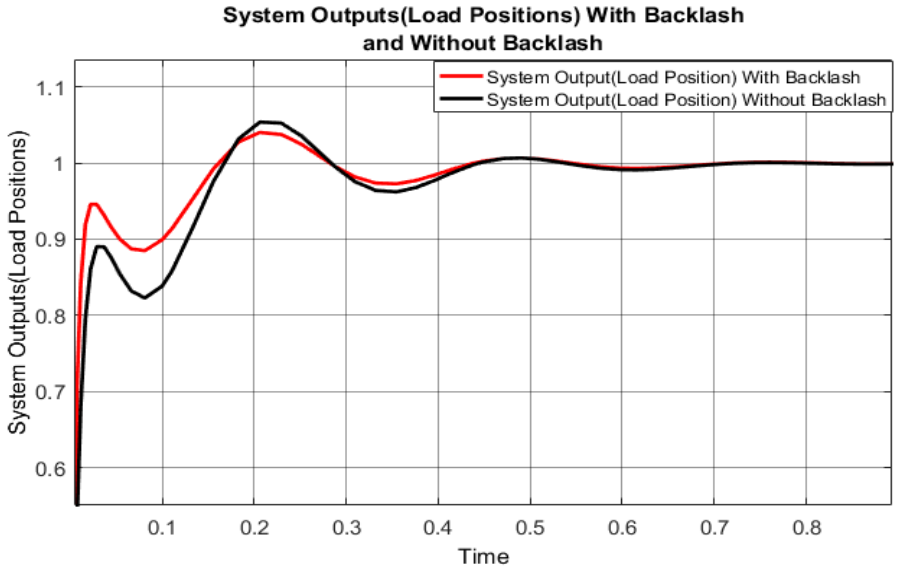

Figure 4.8 System outputs **(**load positions) change: Black line: Load position with backlash, Red line: Load position without backlash – Example.4

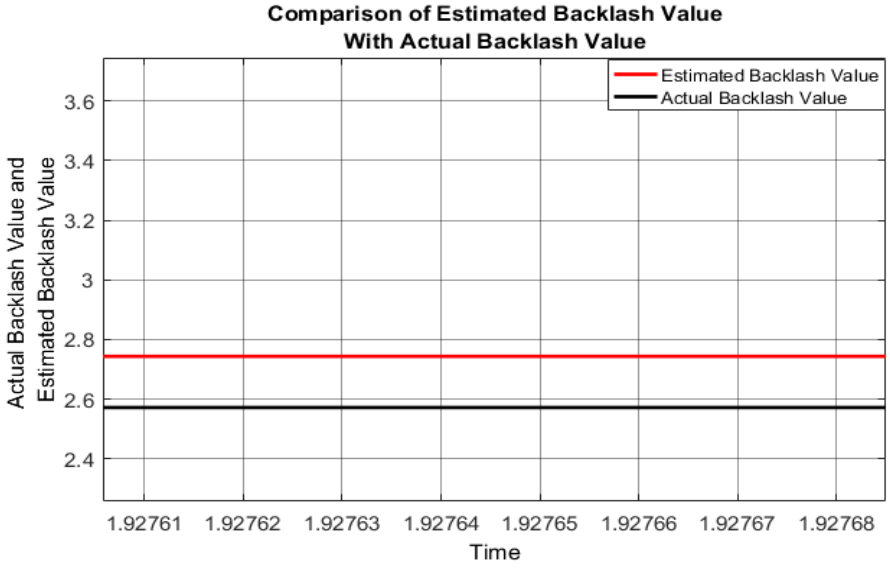

Figure 4.9 Actual backlash size and estimated backlash size: Black line: Actual backlash size, Red line: Estimated backlash size – Example.4

Example 5. System output (load position) with backlash and without backlash is shown in Figure 4.10. Sum of the absolute value of the difference between load positions have been calculated as 1.6×10^{-3}. By using this result, the estimated backlash size has been simulated on the basis of actual backlash size which is 3.0394 (see Figure 4.11) and Band-Limited Noise with zero mean. Estimated backlash size has been identified as 3.164. The difference between actual backlash size and estimated backlash size is 0.1246.

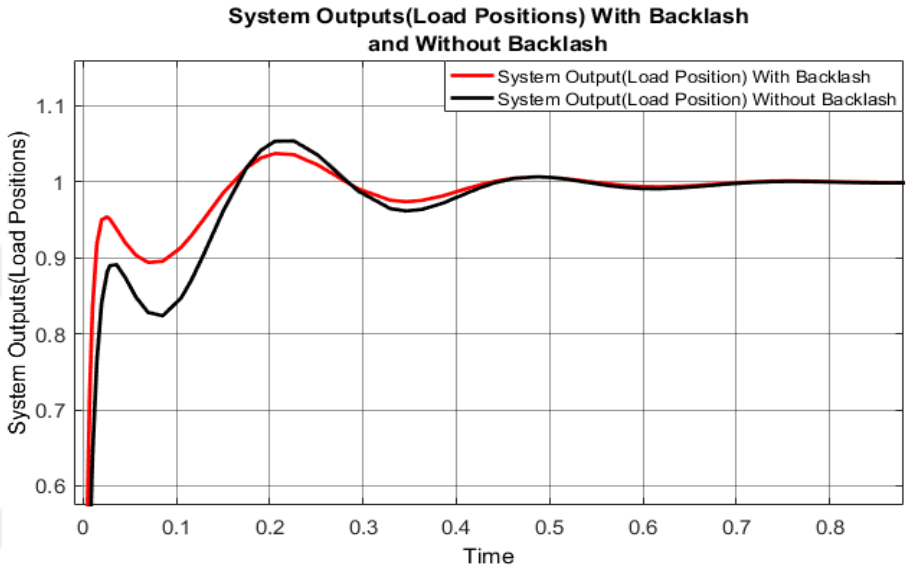

Figure 4.10 System outputs **(**load positions) change: Black line: Load position with backlash, Red line: Load position without backlash – Example.5

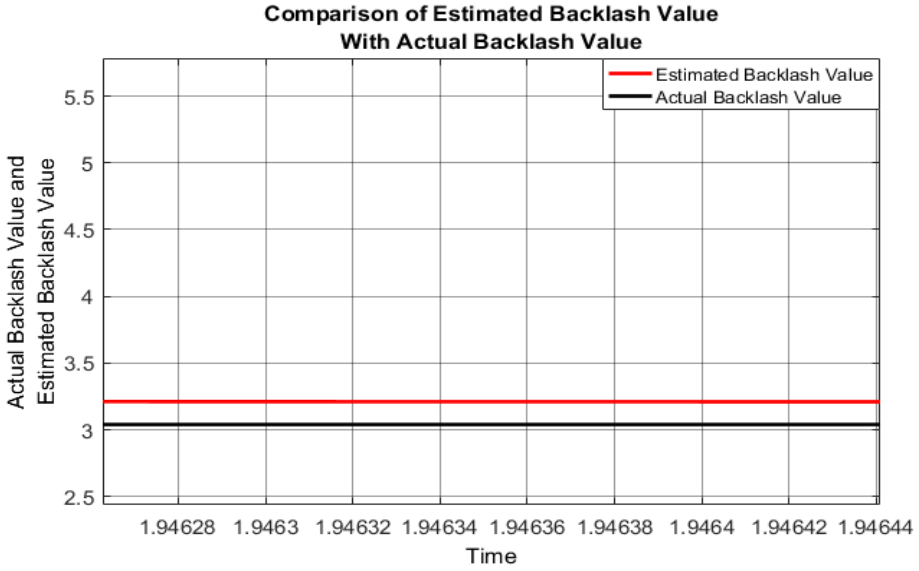

Figure 4.11 Actual backlash size and estimated backlash size: Black line: Actual backlash size, Red line: Estimated backlash size – Example.5

Example 6. System output (load position) with backlash and without backlash is shown in Figure 4.12. Sum of the absolute value of the difference between load positions have been calculated as 1.753×10^{-3}. By using this result, the estimated backlash size has been simulated on the basis of actual backlash size which is 3.6988 (see Figure 4.13) and Band-Limited Noise with zero mean. Estimated backlash size has been identified as 3.624. The difference between actual backlash size and estimated backlash size is 0.0748.

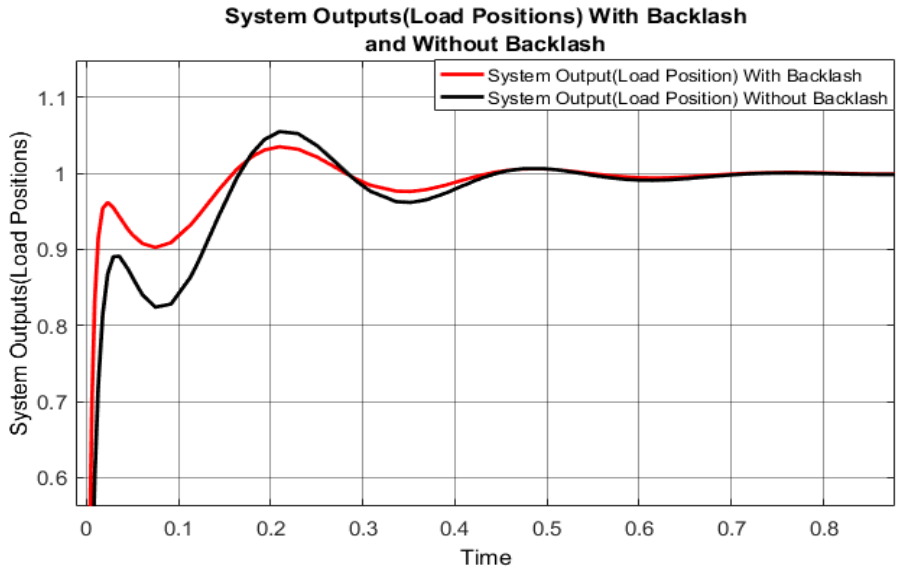

Figure 4.12 System outputs **(**load positions) change: Black line: Load position with backlash, Red line: Load position without backlash – Example.6

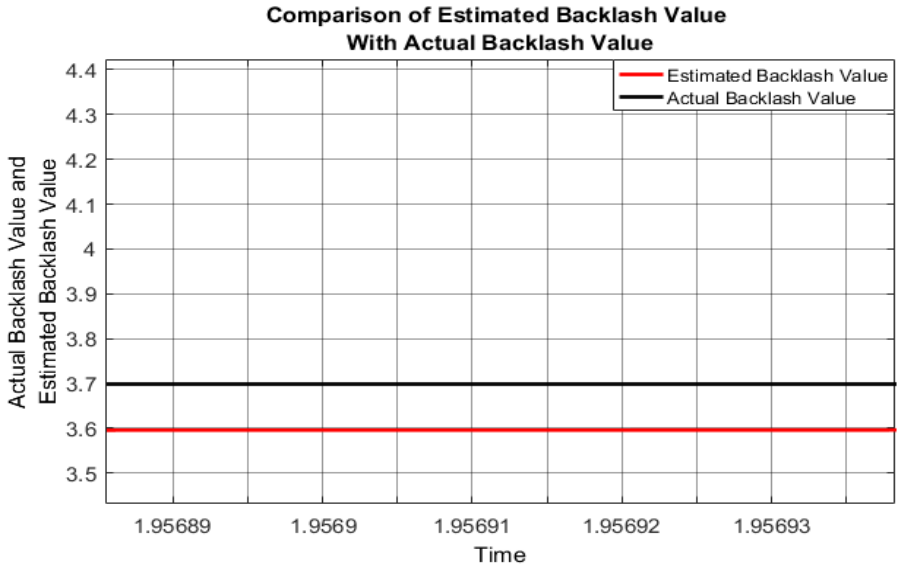

Figure 4.13 Actual backlash size and estimated backlash size: Black line: Actual backlash size, Red line: Estimated backlash size – Example.6

Example 7. System output (load position) with backlash and without backlash is shown in Figure 4.14. Sum of the absolute value of the difference between load positions have been calculated as 1.926×10^{-3}. By using this result, the estimated backlash size has been simulated on the basis of actual backlash size which is 4.2952 (see Figure 4.15) and Band-Limited Noise with zero mean. Estimated backlash size has been identified as 4.196. The difference between actual backlash size and estimated backlash size is 0.0992.

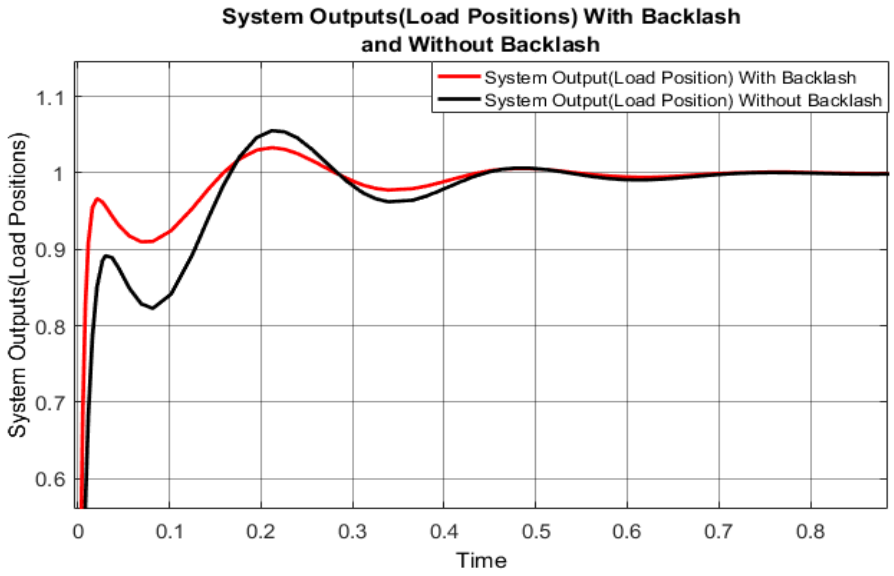

Figure 4.14 System outputs **(**load positions) change: Black line: Load position with backlash, Red line: Load position without backlash – Example.7

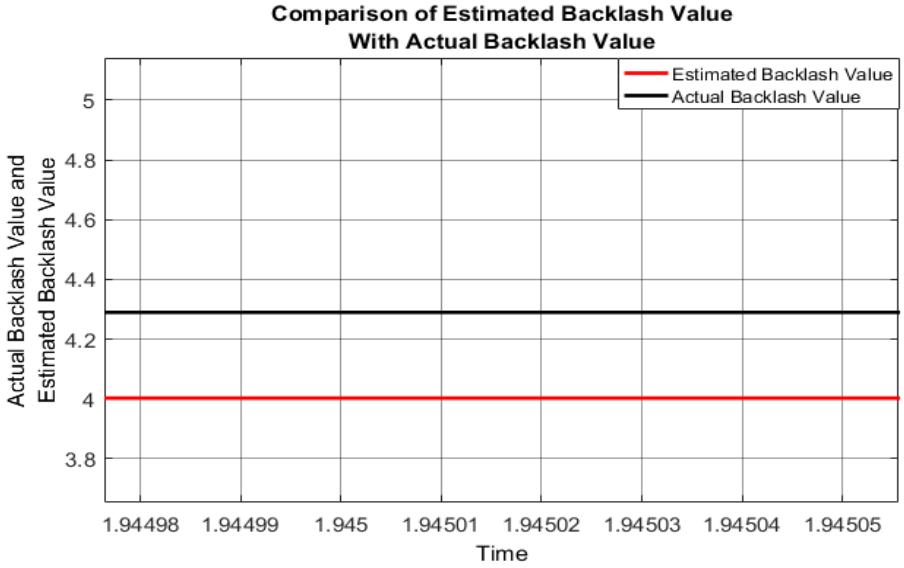

Figure 4.15 Actual backlash size and estimated backlash size: Black line: Actual backlash size, Red line: Estimated backlash size – Example.7

Example 8. System output (load position) with backlash and without backlash is shown in Figure 4.16. Sum of the absolute value of the difference between load positions have been calculated as 2.059×10^{-3}. By using this result, the estimated backlash size has been simulated on the basis of actual backlash size which is 4.7684 (see Figure 4.17) and Band-Limited Noise with zero mean. Estimated backlash size has been identified as 4.679. The difference between actual backlash size and estimated backlash size is 0.0894.

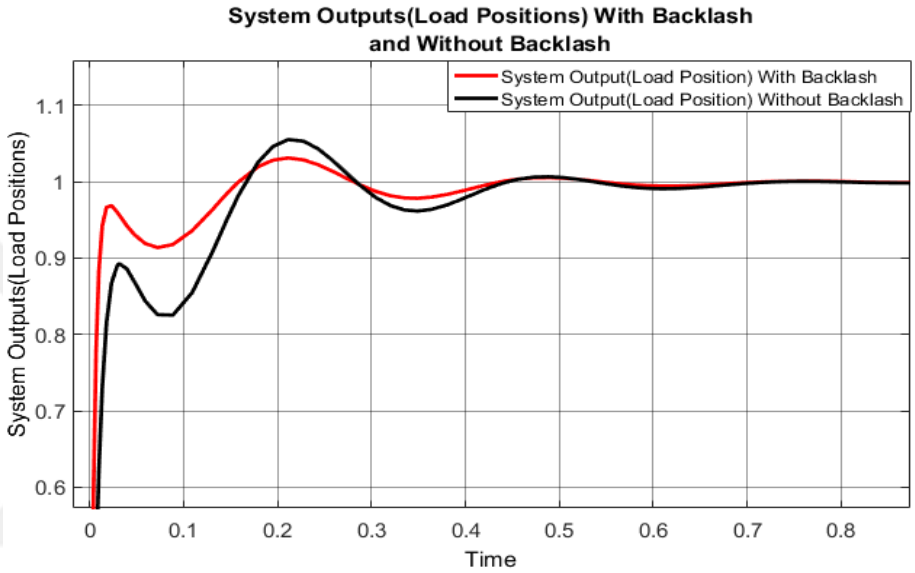

Figure 4.16 System outputs **(**load positions) change: Black line: Load position with backlash, Red line: Load position without backlash – Example.8

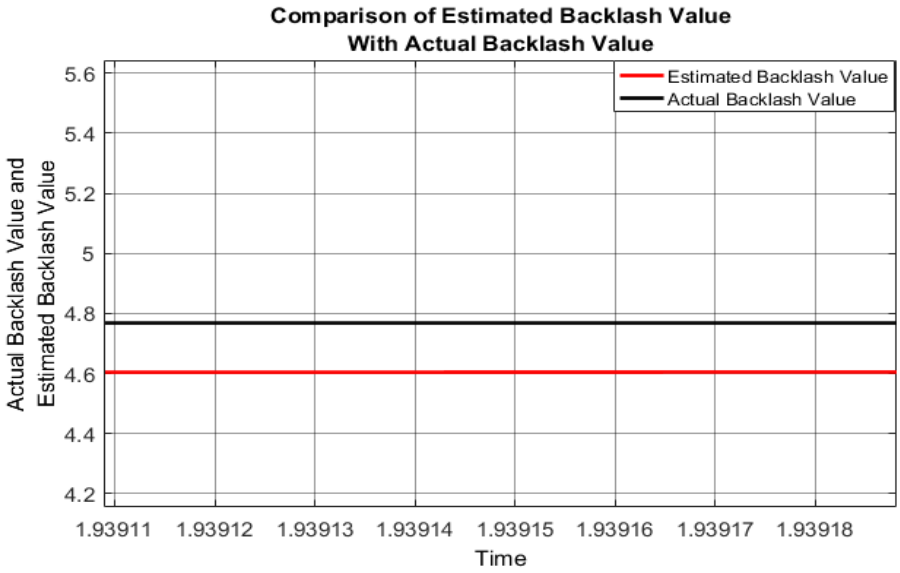

Figure 4.17 Actual backlash size and estimated backlash size: Black line: Actual backlash size, Red line: Estimated backlash size – Example.8

It is expected that there should be a delay when there exists backlash in electromechanical system, but as it is seen in the graphs, the line of load position without backlash (black line) is moving later contrary to expectations. The reason of this delay in the system without backlash (black line) is noise. The size of noise actually has been chosen very small to ignore the effect of noise. However, the chosen value for noise size is not at the desired level. Therefore, the effect of the noise is seen as delay in the system (black line) despite the small size of noise.

4.2 Comparison of Actual Backlash Size and Estimated Backlash Size

Estimated backlash sizes have been obtained for several actual backlash sizes in the system. Table 4.1 shows the estimated backlash size, actual backlash size and the difference between them. Percent error in backlash estimation is also presented in the table as a percentage of the actual backlash size. The error changes between a minimum of 1.87 per cent and a maximum of 5.48 per cent for various backlash sizes.

Table 4.1 Difference between actual backlash size and estimated backlash size

Example number	Actual Backlash Size (α_a)	Estimated Backlash Size (α_e)	The Difference Between Actual Backlash Value and Estimated Backlash Value ($\lvert\alpha_a - \alpha_e\rvert$)	Percent Backlash Estimation Error ($\frac{\lvert\alpha_a-\alpha_e\rvert}{\alpha_a} \times 100\%$)
1	1.2234	1.183	0.0404	3.30%
2	1.7309	1.636	0.0949	5.48%
3	2.3923	2.354	0.0383	1.60%
4	2.5718	2.662	0.0902	3.51%
5	3.0394	3.164	0.1246	4.10%
6	3.6988	3.624	0.0748	2.02%
7	4.2952	4.196	0.0992	2.31%
8	4.7684	4.679	0.0894	1.87%

4.2.1 Mean Square Error

Mean square error has been calculated according to the values shown in Table 4.1 using the following formula:

$$\text{MSE} = \frac{1}{n}\sum \left(actual - estimated \right)^2 \tag{4.1}$$

For n = 8 different backlash sizes and their estimates, MSE value is computed in the following manner.

$$(1.2234 - 1.183)^2 = 1.63216 \times 10^{-3}$$
$$(1.7309 - 1.636)^2 = 9.00601 \times 10^{-3}$$
$$(2.3923 - 2.354)^2 = 1.46689 \times 10^{-3}$$
$$(2.5718 - 2.662)^2 = 8.13604 \times 10^{-3}$$
$$(3.0394 - 3.164)^2 = 0.01552516$$
$$(3.6988 - 3.624)^2 = 5.59504 \times 10^{-3}$$
$$(4.2952 - 4.196)^2 = 9.84064 \times 10^{-3}$$
$$(4.7684 - 4.679)^2 = 7.99236 \times 10^{-3}$$
$$MSE = (1.63216 \times 10^{-3} + 9.00601 \times 10^{-3} + 1.46689 \times 10^{-3} + 8.13604 \times 10^{-3} + 0.01552516 + 5.59504 \times 10^{-3} + 9.84064 \times 10^{-3} + 7.99236 \times 10^{-3})/8$$
$$MSE = 0.0595543/8$$
$$MSE = 7.442875 \times 10^{-3}$$

The value of computed MSE being in the order of 10^{-3} in estimating a series of backlash sizes changing approximately between 1.2 and 4.8 is a clear indication of the success in backlash size estimation.

There are given only 8 examples of simulation results in Table 4.1. However, more than 100 simulation tests have been done during this thesis study. For 100 of these simulation tests average percent backlash estimation error has been obtained as 1.8925% and mean square error (MSE) has been obtained as $9.44395 * 10^{-3}$. The results of the studies in literature are mentioned below.

Lagerberg and Egardt [1, 9, 19] have described the estimators based on Kalman filters for state and size of backlash in their studies. They have measured the backlash size for three different sequences and the values of 0.025 rad, 0.026 rad, 0.027 rad have been obtained respectively. The difference between these sequences is on the order of 5%. Then, Lagerberg and Egardt have compared the estimated backlash size with 0.024 rad which is manually estimated value [1, 9, 19].

Sainio [2] has fitted a powertrain model for a real vehicle and he applied grey-box methods to identify the parameters. Then, several tests have been done with this real electric vehicle. Joonas Sainio has obtained over 90% accuracy in his study when the parametrized model compared to all measured datas [2].

Yang, Tang, Tan and Xu [3] have developed an identification method based upon the integration of speed difference to detect the backlash amplitude automatically in servo transmission system. They have verified the accuracy and effectiveness of the method. In their experimental setup, the given backlash amplitude is 0.035 rad and they have obtained $5.6 * 1e - 4$ rad [3].

Papageorgiou, Blanke, Niemann and Richter [23] have presented a method to estimate the dead-zone angle in a single-axis drive-train with backlash in their work. They have tested the method in simulation and the convergence has been obtained in less than 2 s with precision in the order of 10^{-3} [23].

Dong, Qıngyuan Tan and Yonghong Tan [26] have proposed a pseudo-Wiener model with backlash. By proposing this model, they have aimed on-line identification of dynamic systems with backlash. Ruili Dong, Qıngyuan Tan and Yonghong Tan have obtained $2.62 * 10^{-2}$ maximum relative error in their results [26].

Dong and Tan [28] have suggested an approach for online identification of the sandwich systems with backlash in their study. They have carried out the proposed method to the X-Y moving positioning stage model. After 900 steps, Dong and Tan [28] have achieved the convergence. They have seen that the mean square error (MSE) decrease sharply before 80 steps and then it converges to a constant 0.2 gradually. They have also observed that the maximum relative error is less than %10 [28].

Hägglund [32] has derived an estimation and detection method in order to obtain the amount of backlash automatically by using normal operating datas. Several amounts of backlash, varying from 1% to 10% have been obtained in the results [32].

When the obtained average percent backlash estimation error and mean square error (MSE) for 100 simulation tests are compared with the results of the studies in literature, it is seen that the results are close to each other in general.

CHAPTER V

CONCLUSION AND RECOMMENDATIONS

Two feedback control system models, one of them being for a mechanical system with backlash and the other one for a mechanical system without backlash, have been developed by using computer simulation. The parameters used in state-space form have been introduced and the state-space form has been designed. After designing the state-space form, the augmented system matrix with disturbance (backlash) and noise (ignored or very small size) has been obtained. The controllability and observability of the system have been verified. The constant gain for LQR and the filter gains for system with backlash and without backlash have been formed. Kalman filter has been designed in order to see and understand the effect of the backlash on the load positions more accurately. Sum of the absolute value of the differences between load positions with backlash and load positions without backlash has been obtained. In order to achieve the values of estimated backlash sizes, a mathematical model which is directly proportional with the obtained sum results has been formulated. These calculations and mathematical model have been obtained by using function block in computer simulation library. Estimated backlash values have been obtained by performing simulation experiments for different actual backlash values and their accuracy has been verified.

Finally, percent estimation error has been calculated. The comparison of each estimated backlash size with actual backlash size and percent estimation error for this comparison of backlash sizes have been shown in a table. It has been observed that the simulation study has good results when the values of the estimated backlash sizes are compared with the values of the actual backlash sizes.

Although, there are given a few examples of simulation tests in Chapter IV, many different simulation tests have been done and the average percent backlash estimation error and mean square error (MSE) of these tests have been calculated. When the average percent backlash estimation error and mean square error (MSE) of these simulation tests have been compared with the results of the studies in literature, it is observed that they are generally close to each other.

According to the results, the expected goals have been achieved, but there are some other goals that can be achieved if we continue to work on this subject. For instance, the backlash can be compensated and an experimental setup can be designed in a real system. The presented simulation technique could be useful to create more suitable environment for compensating backlash and designing a control system in future studies. By identifying the backlash size, safety net has been guaranteed for the reliability, functionality and robustness of operating conditions. Therefore, it can eliminate the effects of backlash which limit the performance of speed and position control in industrial, robotics, automotive and other applications. In addition, it can be used for more complex systems with backlash.

5.1 Recommendations for Future Work

There are some recommendations for future work to strengthen the findings obtained in this study. In this thesis study, backlash size has been identified by observing load position based on Kalman filter method. In addition to the Kalman state observer, there are also several methods can be used to identify the backlash size. The first method is that backlash size could be obtained by integrating the speed difference. The second method is quasi-stationary state identification method. Another method is that backlash size can be identified based upon the increasing pulse of the torque. One more method that can be used is similar to the previous one, where the backlash size could be obtained by using the approach based on the small pulse of the torque [3].

Backlash has an important role especially in the industrial sector in which there are many mechanical systems. However, only the identification of the backlash size is not sufficient. If the size and location of the backlash are not known when backlash

exists in a mechanical system, the whole of the mechanism or system sometimes needs to be replaced. Such a problem is seen generally in the industrial sector, which results in a decrease of productivity. As an outcome of this thesis study, the size of the backlash has been identified. If a method can be developed for determining the location of the backlash, the problem could be solved. Instead of the whole mechanism, only the backlash part of the mechanism will be sufficient to be replaced. Thus, the negative effects of backlash on the productivity especially in the industrial sector will be reduced significantly.

The identification of the backlash size has been discussed in this thesis study in computer simulation environment. In order to obtain more realistic results, the same study might be made by designing an experimental setup. After identifying the backlash using the approach proposed here, some new methods could be developed to compensate the active backlash as a continuation of this thesis study. Thus, the effects which occur due to the backlash can be eliminated and the system performances can be controlled and improved.

If the nature and effects of the backlash can be fully understood and represented with all details and if the methods for identifying and compensating the backlash can be developed at the desired level, significant improvements in efficacy of electromechanical systems in the sectors of robotics, automation and industrial production can be achieved.

REFERENCES

[1] Lagerberg, A., & Egardt, B. (2007). Backlash Estimation with aApplication to Automotive Powertrains. *IEEE Transactions on Control Systems Technology*, **15(3)**, 483-493.

[2] Sainio, J. (2016). Backlash Compensation in Electric Vehicle Powertrain.

[3] Yang, M., Tang, S., Tan, J., & Xu, D. (2012). Study of On-line Backlash Identification for PMSM Servo System. *IECON 2012-38th Annual Conference on IEEE Industrial Electronics Society,* 2036-2042 IEEE.

[4] Vörös, J. (2010). Modeling and Identification of Systems with Backlash. *Automatica,* **46(2)**, 369-374.

[5] Nordin, M., & Gutman, P. O. (2002). Controlling Mechanical Systems with Backlash—a Survey. *Automatica*, **38(10)**, 1633-1649.

[6] Haventon, M., & Öberg, J. (2008). Testing and Implementation of a Backlash Detection Algorithm. *M.Sc. Thesis*.

[7] Brunton, S. L., & Kutz, J. N. (2019). *Data-driven Science and Engineering: Machine Learning, Dynamical Systems, and Control*. Cambridge University Press.

[8] Nordin, M., Galic', J., & Gutman, P. O. (1997). New Models for Backlash and Gear Play. *International Journal of Adaptive Control and Signal Processing*, **11(1)**, 49-63.

[9] Lagerberg, A. (2004). *Control and Estimation of Automotive Powertrains with Backlash* (Doctoral Dissertation, Department of Signals and Systems, Chalmers University of Technology).

[10] Jukić, T., & Perić, N. (2003, September). A Comparative Study of Backlash Compensation Methods. In *2003 European Control Conference (ECC)*, 3261-3266 IEEE.

[11] Acho, L., Ikhouane, F., & Pujo, G. (2013). Robust Control Design for Mechanisms with Backlash. *Journal of Control Engineering and Technology*, **3(4)**, 175-180.

[12] Mola, M., Khayatian, A., & Dehghani, M. (2013, May). Identification and Adaptive Position Control of Two Mass Systems with Unknown Backlash. In *2013 21st Iranian Conference on Electrical Engineering (ICEE)*, 1-6 IEEE.

[13] Reyland Jr, J., & Bai, E. W. (2014). Generalized Wiener System Identification: General Backlash Nonlinearity and Finite Impulse Response Linear Part. *International Journal of Adaptive Control and Signal Processing*, **28(11)**, 1174-1188.

[14] Tarbouriech, S., Queinnec, I., & Prieur, C. (2013, December). Stability Analysis for Systems with Saturation and Backlash in the Loop. In *52nd IEEE Conference on Decision and Control*, 6652-6657 IEEE.

[15] Sarkar, N., Ellis, R. E., & Moore, T. N. (1997). Backlash Detection in Geared Mechanisms: Modeling, Simulation, and Experimentation. *Mechanical systems and signal processing*, **11(3)**, 391-408.

[16] Barreiro, A., & Baños, A. (2006). Input–output Stability of Systems with Backlash. *Automatica*, **42(6)**, 1017-1024.

[17] Hovland, G., Hanssen, S., Gallestey, E., Moberg, S., Brogardh, T., Gunnarsson, S., & Isaksson, M. (2002, October). Nonlinear Identification of Backlash in Robot Transmissions. In *Proceedings of the 33rd ISR (International Symposium on Robotics)*, 1-6

[18] Yumrukçal, Z. (2013). *Dynamic Modeling of High Precision Servo Systems with Gear Backlash* (Doctoral Dissertation, PhD Thesis, MIDDLE EAST TECHNICAL UNIVERSITY).

[19] Lagerberg, A., & Egardt, B. S. (2003, December). Estimation of Backlash with Application to Automotive Powertrains. In *42nd IEEE International Conference on Decision and Control (IEEE Cat. No. 03CH37475)*, Vol. 5, 4521-4526, IEEE.

[20] Tao, G., & Kokotovic, P. V. (1995). Adaptive Control of System with Unknown Output Backlash. *IEEE Transactions on Automatic Control*, **40(2)**, 326-330.

[21] Tao, G., & Kokotović, P. V. (1997). Adaptive Control of Systems with Unknown Non-smooth Non-linearities. *International journal of adaptive control and signal processing*, **11(1)**, 81-100.

[22] Cerone, V., & Regruto, D. (2007). Bounding the Parameters of Linear Systems with Input Backlash. *IEEE Transactions on Automatic Control*, **52(3)**, 531-536.

[23] Papageorgiou, D., Blanke, M., Niemann, H. H., & Richter, J. H. (2017). Backlash Estimation for Industrial Drive-train Systems. *IFAC-PapersOnLine*, **50(1)**, 3281-3286.

[24] Ruderman, M., Hoffmann, F., & Bertram, T. (2009). Modeling and Identification of Elastic Robot Joints with Hysteresis and Backlash. *IEEE Transactions on Industrial Electronics*, **56(10)**, 3840-3847.

[25] Wang, X. S., Su, C. Y., & Hong, H. (2004). Robust Adaptive Control of a Class of Nonlinear Systems with Unknown Dead-zone. *Automatica*, **40(3)**, 407-413.00

[26] Dong, R., Tan, Q., & Tan, Y. (2009). Recursive Identification Algorithm for Dynamic Systems with Output Backlash and its Convergence. *International Journal of Applied Mathematics and Computer Science*, **19(4)**, 631-638.

[27] Cerone, V., Piga, D., & Regruto, D. (2009). Parameter Bounds Evaluation for Linear System with Output Backlash. *IFAC Proceedings Volumes*, **42(10)**, 575-580.

[28] Dong, R., & Tan, Y. (2011). On-line Identification Algorithm and Convergence Analysis for Sandwich Systems with Backlash. *International Journal of Control, Automation and Systems*, **9(3)**, 588-594.

[29] Vörös, J. (2014). Modeling and Identification of Nonlinear Cascade and Sandwich Systems with General Backlash. *Journal of Electrical Engineering*, **65(2)**, 104-110.

[30] Lagerberg, A. (2001). *A Literature Survey on Control of Automotive Powertrains with Backlash*. Chalmers Tekniska Högsk..

[31] Ezal, K., Kokotovic, P. V., & Tao, G. (1997, December). Optimal Control of Tracking Systems with Backlash and Flexibility. In *Proceedings of the 36th IEEE Conference on Decision and Control*, Vol. 2, 1749-1754, IEEE.

[32] Hägglund, T. (2007). Automatic On-line Estimation of Backlash in Control Loops. *Journal of Process Control*, **17(6)**, 489-499.

[33] Grundelius, M., & Angeli, D. (1996, December). Adaptive Control of Systems with Backlash Acting on the Input. In *Proceedings of 35th IEEE Conference on Decision and Control*, Vol. 4, 4689-4694, IEEE.

[34] Angeli, D. (1996). Adaptive Control of Systems with Backlash. *MSc Thesis*.

[35] Merzouki, R., Davila, J. A., Fridman, L., & Cadiou, J. C. (2007). Backlash Phenomenon Observation and Identification in Electromechanical System. *Control Engineering Practice*, **15(4)**, 447-457.

APPENDIX

PARAMETER ESTIMATION RELATED DATA

The parameters which are mentioned in Chapter III have been obtained via computer programming language. There will be given the results of these parameters which are state-space system with backlash and noise for load side ($sysCl$), state-space models for Kalman filter with backlash ($sysKFL$) and without backlash ($sysKFLNO$).

The state-space system with backlash and noise(ignored or very small) for load side has been obtained as:

$sysCl = ss(A, BF, Cl, [0\ 0\ 0\ 0\ 0\ 0\ 0\ V_n])$

```
sysCl =

 A =
          x1        x2        x3        x4        x5        x6
  x1        0         1         0         0         0         0
  x2   -519.8     -5.73      2071    0.6275         0       2.5
  x3        0         0         0         1         0         0
  x4    147.9   0.04482    -589.3   -0.3571   -0.1786         0
  x5        0         0         0         0         0         0
  x6        0         0         0         0         0        -1

 B =
         u1      u2      u3      u4      u5      u6      u7      u8
  x1      0   4.488       0       0       0       0       0       0
  x2      0       0   4.488       0       0       0       0       0
  x3      0       0       0   4.488       0       0       0       0
  x4      0       0       0       0   4.488       0       0       0
  x5      0       0       0       0       0   4.488       0       0
  x6      1       0       0       0       0       0   4.488       0

 C =
      x1  x2  x3  x4  x5  x6
  y1   0   0   1   0   0   0

 D =
         u1      u2      u3      u4      u5      u6      u7      u8
  y1      0       0       0       0       0       0       0  0.0001
```

Figure A.1 State-space system with backlash and noise (ignored or very small) for load side

The state-space models for Kalman filter with backlash and without backlash have been designed. The model with backlash has been obtained as follows:

$$sysKFL = ss(A - Kfl * Cl, [B\ Kfl],\ eye(6),\ 0 * [B\ Kfl])$$

```
>> sysKFL

sysKFL =

  A =
           x1        x2        x3        x4        x5        x6
   x1        0         1    -13.66         0         0         0
   x2   -519.8     -5.73      2533    0.6275         0       2.5
   x3        0         0    -214.2         1         0         0
   x4    147.9   0.04482     -1094   -0.3571   -0.1786         0
   x5        0         0     211.8         0         0         0
   x6        0         0     -22.3         0         0        -1

  B =
          u1       u2
   x1      0    13.66
   x2      0     -462
   x3      0    214.2
   x4      0    504.5
   x5      0   -211.8
   x6      1     22.3

  C =
       x1  x2  x3  x4  x5  x6
   y1   1   0   0   0   0   0
   y2   0   1   0   0   0   0
   y3   0   0   1   0   0   0
   y4   0   0   0   1   0   0
   y5   0   0   0   0   1   0
   y6   0   0   0   0   0   1

  D =
       u1  u2
   y1   0   0
   y2   0   0
   y3   0   0
   y4   0   0
   y5   0   0
   y6   0   0
```

Figure A.2 State-space model for Kalman filter with backlash

The state-space model for Kalman filter without backlash has been obtained as:

$$sysKFLNO = ss(A - Kflno * Cl, [B\ Kflno],\ eye(6),\ 0 * [B\ Kflno])$$

```
>> sysKFLNO

sysKFLNO =

  A =
              x1         x2         x3         x4         x5         x6
   x1          0          1     -8.129          0          0          0
   x2     -519.8     -5.73       1698     0.6275          0        2.5
   x3          0          0     -100.7          1          0          0
   x4      147.9    0.04482       -657    -0.3571    -0.1786          0
   x5          0          0        100          0          0          0
   x6          0          0     -10.44          0          0         -1

  B =
          u1       u2
   x1      0    8.129
   x2      0    372.4
   x3      0    100.7
   x4      0    67.71
   x5      0     -100
   x6      1    10.44

  C =
       x1  x2  x3  x4  x5  x6
   y1   1   0   0   0   0   0
   y2   0   1   0   0   0   0
   y3   0   0   1   0   0   0
   y4   0   0   0   1   0   0
   y5   0   0   0   0   1   0
   y6   0   0   0   0   0   1

  D =
       u1  u2
   y1   0   0
   y2   0   0
   y3   0   0
   y4   0   0
   y5   0   0
   y6   0   0
```

Figure A.3 State-space model for Kalman filter without backlash

CIRRICULUM VITAE (CV)

PERSONAL INFORMATION

Name and Surname: Mehmet Fatih ÇAKAR

Nationality: Turkish

EDUCATION INFORMATION

	Graduated school	Graduation year
Master Degree	Gaziantep University	Present
Bachelor Degree	Gaziantep University	2017
High School	Zeve Anatolian High School	2012

WORK EXPERIENCE

	Duty
2020-Still	Research Assistant in İstanbul Aydın University
2018-2020	Electrical and Electronics Engineer in Reform Environmental Occupational Safety Measurement Test Analysis Laboratory (Gaziantep)
2017-2018	Maintenance Engineer in Artos Elevator (Van)

PUBLICATIONS

Çakar, A. G. M. F. & Kara, T. ELEKTROMEKANİK SİSTEMLERDEKİ MEKANİK BOŞLUĞUN KONTROL AMAÇLI TANILANMASI, Karadeniz Zirvesi 4. Uluslararası Uygulamalı Bilimler Kongresi

LANGUAGE SKILLS

English Reading: Good Writing: Advanced Speaking: Good

HOBBIES

Ping-Pong (Table Tennis), Football, Reading, Swimming, Chess